

University of Minho
School of Engineering

José Nuno Martins da Costa

**Modular framework for a breast biopsy
smart navigation system**



University of Minho
School of Engineering

José Nuno Martins da Costa

**Modular framework for a breast biopsy
smart navigation system**

Masters Dissertation
Master's in Informatics Engineering

Dissertation supervised by
Victor Manuel Rodrigues Alves
João Luís Araújo Martins Vilaça

Copyright and Terms of Use for Third Party Work

This dissertation reports on academic work that can be used by third parties as long as the internationally accepted standards and good practices are respected concerning copyright and related rights.

This work can thereafter be used under the terms established in the license below.

Readers needing authorization conditions not provided for in the indicated licensing should contact the author through the RepositóriUM of the University of Minho.

License granted to users of this work:



CC BY-NC

<https://creativecommons.org/licenses/by-nc/4.0/>

Acknowledgements

I would like to thank my supervisors and colleagues at the 2Ai-lab in the Polytechnic Institute of Cavado and Ave for the opportunity and the knowledge I acquired in the last year.

A special thanks to my supervisor at the University of Minho, Victor Alves, for all the help and advice in this dissertation.

I would like to thank all the knowledge, help, and advice from all the wonderful people I've met in my academic journey.

I would also like to give a special mention to the Tuna de Medicina da Universidade do Minho, for despite my late entry still gave me some of my best academic times.

To my girlfriend and friends that were always at my side hearing my complaints and my jokes.

Finally, I would like to thank my parents and my family for all the support and advice on this journey.

Statement of Integrity

I hereby declare having conducted this academic work with integrity.

I confirm that I have not used plagiarism or any form of undue use of information or falsification of results along the process leading to its elaboration.

I further declare that I have fully acknowledged the Code of Ethical Conduct of the University of Minho.

University of Minho, Braga, october 2022

José Nuno Martins da Costa

Abstract

Breast cancer is currently one of the most commonly diagnosed cancers and the fifth leading cause of cancer-related deaths. Its treatment has a higher survivorship rate when diagnosed in the disease's early stages. The screening procedure uses medical imaging techniques, such as mammography or ultrasound, to discover possible lesions. When a physician finds a lesion that is likely to be malignant, a biopsy is performed to obtain a sample and determine its characteristics. Currently, real-time ultrasound is the preferred medical imaging modality to perform this procedure. The breast biopsy procedure is highly reliant on the operator's skill and experience, due to the difficulty in interpreting ultrasound images and correctly aiming the needle. Robotic solutions, and the usage of automatic lesion segmentation in ultrasound imaging along with advanced visualization techniques, such as augmented reality, can potentially make this process simpler, safer, and faster.

The OncoNavigator project, in which this dissertation integrates, aims to improve the precision of the current breast cancer interventions. To accomplish this objective various medical training and robotic biopsy aid were developed. An augmented reality ultrasound training solution was created and the device's tracking capabilities were validated by comparing it with an electromagnetic tracking device. Another solution for ultrasound-guided breast biopsy assisted with augmented reality was developed. This solution displays real-time ultrasound video, automatic lesion segmentation, and biopsy needle trajectory display in the user's field of view. The validation of this solution was made by comparing its usability with the traditional procedure. A modular software framework was also developed that focuses on the integration of a collaborative medical robot with real-time ultrasound imaging and automatic lesion segmentation. Overall, the developed solutions offered good results. The augmented reality glasses tracking capabilities proved to be as capable as the electromagnetic system, and the augmented reality assisted breast biopsy proved to make the procedure more accurate and precise than the traditional system.

Keywords Breast Cancer, Breast Biopsy, Ultrasound, OncoNavigator, Augmented Reality

Resumo

O cancro da mama é, atualmente, um dos tipos de cancro mais comuns a serem diagnosticados e a quinta principal causa de mortes relacionadas ao cancro. O seu tratamento tem maior taxa de sobrevivência quando é diagnosticado nas fases iniciais da doença. O procedimento de triagem utiliza técnicas de imagem médica, como mamografia ou ultrassom, para descobrir possíveis lesões. Quando um médico encontra uma lesão com probabilidade de ser maligna, é realizada uma biópsia para obter uma amostra e determinar as suas características. O ultrassom em tempo real é a modalidade de imagem médica preferida para realizar esse procedimento. A biópsia mamária depende da habilidade e experiência do operador, devido à dificuldade de interpretação das imagens ultrassonográficas e ao direcionamento correto da agulha. Soluções robóticas, com o uso de segmentação automática de lesões em imagens de ultrassom, juntamente com técnicas avançadas de visualização, nomeadamente realidade aumentada, podem tornar esse processo mais simples, seguro e rápido.

O projeto OncoNavigator, que esta dissertação integra, visa melhorar a precisão das atuais intervenções ao cancro da mama. Para atingir este objetivo, várias ajudas para treino médico e auxílio à biópsia por meio robótico foram desenvolvidas. Uma solução de treino de ultrassom com realidade aumentada foi criada e os recursos de rastreio do dispositivo foram validados comparando-os com um dispositivo eletromagnético. Outra solução para biópsia de mama guiada por ultrassom assistida com realidade aumentada foi desenvolvida. Esta solução exibe vídeo de ultrassom em tempo real, segmentação automática de lesões e exibição da trajetória da agulha de biópsia no campo de visão do utilizador. A validação desta solução foi feita comparando a sua usabilidade com o procedimento tradicional. Também foi desenvolvida uma estrutura de software modular que se concentra na integração de um robô médico colaborativo com imagens de ultrassom em tempo real e segmentação automática de lesões. Os recursos de rastreio dos óculos de realidade aumentada mostraram-se tão capazes quanto o sistema eletromagnético, e a biópsia de mama assistida por realidade aumentada provou tornar o procedimento mais exato e preciso do que o sistema tradicional.

Palavras-chave Cancro da Mama, Biópsia Mamária, Ultrassom, OncoNavigator, Realidade Aumentada

Contents

- 1 Introduction 1**
 - 1.1 Breast Cancer 1
 - 1.2 Current Diagnostic Techniques 2
 - 1.3 OncoNavigator Project 5
 - 1.4 Medical Navigation Systems 6
 - 1.5 Robot Assisted Breast Biopsy 7
 - 1.6 Robot Communication Protocols 7
 - 1.7 Motivation 9
 - 1.8 Research Questions 9
 - 1.9 Objectives 10
 - 1.10 Dissertation Structure 12

- 2 Ultrasound training simulator using augmented reality glasses: an accuracy and precision assessment study 13**
 - 2.1 Introduction 14
 - 2.2 Methods and Techniques 16
 - 2.2.1 Overview 16
 - 2.2.2 QR Code Tracking 17
 - 2.2.3 US Simulator 17
 - 2.2.4 Communication 17
 - 2.3 Experiments 18
 - 2.3.1 Experimental Setup 18
 - 2.3.2 Orientation Accuracy and Precision 18
 - 2.4 Results 20
 - 2.4.1 Orientation Accuracy and Precision 20

2.5	Discussion	21
2.6	Conclusion	21
3	Augmented reality-assisted ultrasound breast biopsy	22
3.1	Introduction	24
3.2	Methods and Techniques	25
3.2.1	Overview	25
3.2.2	Companion Application	26
3.2.3	AR Application	28
3.3	Experiments	31
3.3.1	Latency and Execution Times	31
3.3.2	Usability	31
3.4	Results	33
3.4.1	Latency and Execution Times	33
3.4.2	Usability	33
3.5	Discussion	34
3.6	Conclusion	35
4	Proof-of-concept ultrasound biopsy application	37
4.1	Introduction	37
4.2	Developed Features	38
4.2.1	Ultrasound Specific	38
4.2.2	Collaborative Robot Control	41
4.2.3	Usability	42
4.3	Discussion	46
5	Conclusion	48

List of Figures

- 1 Anatomy of a woman's breast. Retrieved from [1]. 1
- 2 Images of an approximately 40mm invasive breast cancer. A - Mammography, B - Ultra-
sound, C - Magnetic Resonance Imaging. Retrieved from [2]. 4
- 3 A and B - Ultrasound imaging of the needle obtaining a sample. C - Breast biopsy
procedure representation. Retrieved from [3]. 4
- 4 OncoNavigator project overview. 5
- 5 TCP and UDP workflows. 9
- 6 Use case 1 and 2 compared with the overarching OncoNavigator framework. 10
- 7 Use case 3 compared with the overarching OncoNavigator framework. 11
- 8 Overview of the proposed framework. 15
- 9 View from HoloLens display showing the US image over the QR code assembled at the
top of the portable US probe. 16
- 10 The 6 different orientations tested during accuracy and precision assessment. 19
- 11 Measured rotation along the probe's central axis represented by θ on the left. Movements
used to calculate accuracy represented by α on the right. 19
- 12 Overview of the different components of the proposed prototype. 26
- 13 Companion application workflow overview. 28
- 14 User's point of view performing the biopsy procedure with the AR device. 29
- 15 Latency test setup, showing in picture A the optical marker mounted on the US probe, in
picture B the breast phantom with both positions marked, and in pictures C and D the
US probe in its different test positions. 32
- 16 Third-person usability test view of a user performing the biopsy in a breast phantom. . . 32
- 17 Latency and Execution times. 33
- 18 Procedure time, distance from the needle tip to the lesion and angle measurements. . . 34

19	Screenshot of the application's GUI.	37
20	GUI US connection settings	38
21	GUI changes when connected to the US probe.	39
22	US connection workflow diagram.	39
23	US image reception workflow diagram.	39
24	Depth slider user interface and the respective resulting US images.	40
25	Depth change workflow diagram.	40
26	Gain setting buttons.	41
27	Gain change workflow diagram.	41
28	Robot control workflow diagram.	42
29	Segmentation overlay feature.	42
30	Segmentation activation workflow diagram.	43
31	Video recording and image screenshot setting options.	43
32	Video recording in practice.	44
33	Recording process start workflow diagram.	44
34	End recording workflow diagram.	45
35	Screenshot workflow diagram.	45
36	Distance widget display.	46
37	Distance tool activation workflow diagram.	46

List of Tables

- 1 Risk factors related to breast cancer worldwide adapted from [4]. 3
- 2 Orientation accuracy measured between different positions (Mean \pm Standard Deviation). 20
- 3 Orientation precision measured at each position (Mean \pm Standard Deviation). 20

Acronyms

API Application Programming Interface. [26](#), [27](#), [38](#), [41](#), [42](#)

AR Augmented Reality. [9](#), [10](#), [11](#), [14](#), [15](#), [16](#), [17](#), [21](#), [23](#), [24](#), [25](#), [26](#), [27](#), [28](#), [29](#), [30](#), [31](#), [33](#), [34](#), [35](#), [48](#), [49](#)

CNN Convolutional Neural Networks. [24](#), [25](#), [26](#), [27](#), [28](#), [30](#), [31](#), [33](#), [34](#), [35](#)

EMT Electromagnetic Tracking. [15](#), [18](#)

FPS Frames per Second. [17](#), [43](#), [44](#), [46](#)

GPU Graphical Processing Unit. [26](#), [27](#)

GUI Graphical User Interface. [7](#), [27](#), [37](#)

IP Internet Protocol. [7](#), [17](#), [38](#)

MG Mammography. [2](#), [3](#), [24](#)

MRI Magnetic Resonance Imaging. [2](#), [3](#), [6](#)

TCP Transmission Control Protocol. [8](#), [17](#), [27](#)

UDP User Datagram Protocol. [8](#), [18](#), [27](#), [28](#), [30](#)

US Ultrasound. [2](#), [3](#), [5](#), [6](#), [7](#), [9](#), [10](#), [11](#), [12](#), [14](#), [15](#), [16](#), [17](#), [18](#), [21](#), [23](#), [24](#), [25](#), [26](#), [27](#), [28](#), [29](#), [30](#), [31](#), [33](#), [34](#), [35](#), [37](#), [38](#), [40](#), [41](#), [42](#), [43](#), [44](#), [45](#), [46](#), [47](#), [48](#)

Chapter 1

Introduction

1.1 Breast Cancer

The human breast is a modified cutaneous exocrine gland made up of skin and subcutaneous tissue, breast parenchyma (ducts and lobules), and supporting stroma, which includes fat; all interconnected by a complex network of ligaments, nerves, arteries and veins, and lymphatics (Figure 1). Breast boundaries in both men and women normally stretch from the second rib superiorly to the sixth rib inferiorly, with the sternum medially and the midaxillary line laterally.

In contrast to the male breast, which is almost entirely made up of fat, the female breast is frequently larger and contains more fibroglandular tissue [5]. Tumors tend to form on the breast parenchyma, inside lobes and ducts, so the female breast is more vulnerable to them [1].

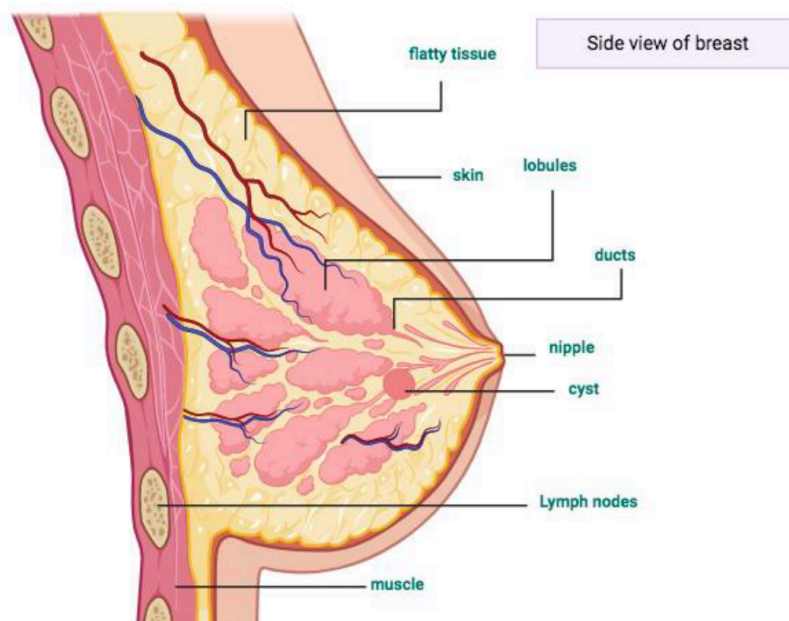


Figure 1: Anatomy of a woman's breast. Retrieved from [1].

With an estimated 2.3 million new cases worldwide in 2020, breast cancer is currently one of the most commonly diagnosed cancers, when excluding nonmelanoma skin cancer, and the fifth leading cause of cancer-related deaths. Globally, breast cancer was responsible for 684,996 deaths in 2020, making it the leading cause of cancer death in women. Although developed regions had the highest incidence rates, 63% of all deaths worldwide in 2020 occurred in Asia and Africa. Breast cancer survivorship rates are higher for women in high-income countries than they are for those in many low and middle-income nations. Even though a considerable portion of cancers do not always result in death, they significantly reduce the quality of life and generally result in higher costs [6].

Highly developed countries like Belgium, Denmark, Australia, the USA, the United Kingdom, and Italy, had much higher incidence rates (95.4 per 100,000 population) compared to the world's age-standardized incidence rates (47.8 per 100,000 population) [7]. This phenomenon is a result of a long-standing higher prevalence of risk factors, including continued fertility decline, high rates of oral contraceptive or hormonal menopausal therapy use, decreased breastfeeding time and increased body weight. Aging and population growth were also key drivers of the rapidly rising burden of breast cancer [4]. A comprehensive table with breast cancer risk factors are shown in Table 1.

1.2 Current Diagnostic Techniques

Breast cancer treatment is more effective in the early stages of the disease, so an emphasis on screening has been adopted by many countries in the world [8]. As a result of these measures, the survival rate of breast cancer is increasing with a 5-year survival rate of 89% between 2005 and 2011 [9].

Breast cancer screening seeks to detect potential malignant lesions before possible symptoms appear, intending to reduce mortality through early intervention. There are various screening methods available, including Mammography (MG), Ultrasound (US), Magnetic Resonance Imaging (MRI) (Figure 2) [10]. MG and US are the most commonly used imaging modalities for lesion screening before they become invasive [1].

On all breast imaging modalities, including MG and other x-ray methods (including tomosynthesis and contrast-enhanced MG), US, and MRI, several benign abnormalities can mimic malignant abnormalities. Even with the most recent improvements in breast imaging, tissue sampling is still the most reliable way to confirm or rule out malignancy [11]. Evidence suggests that non-imaging-guided free-hand procedures have lower sensitivity than image-guided procedures, while US-guided and MG-guided biopsies have sensitivity and specificity comparable to surgical biopsies with fewer adverse events. Percutaneous

Table 1: Risk factors related to breast cancer worldwide adapted from [4].

	Risk Factors	Protective	Predisposing
Demographic	Female gender		✓
	Age		✓
Reproductive	Late age of menopause		✓
	Full-term pregnancy	✓	
	Ovulatory menstrual cycle	✓	
	Pregnancy characteristics	✓	✓
Hormonal	Hormonal contraceptive methods		✓
	Postmenopausal hormone therapy		✓
Hereditary	Genetic factors		✓
	Positive family history of breast cancer		✓
Breast Related	Lesser lactation duration	✓	
	Benign breast disorders		✓
	Obesity and overweight		✓
Lifestyle	Alcohol consumption		✓
	Smoking		✓
	Diet		✓
	Physical activity	✓	
	Vitamin D	✓	
Others	Air pollution		✓
	Socioeconomic status		✓
	Diabetes		✓
	Radiation		✓

image-guided biopsy has, therefore, replaced surgical biopsy allowing a minimally-invasive safe, accurate, and cost-effective diagnosis of breast lesions, necessary for the definition of treatment planning [12].

Needle biopsies are guided by either US, MG, or MRI. Among these, US is the most extensively applied imaging technique due to its real-time capabilities and cost-effectiveness (Figure 3). This being said, US is heavily operator dependent and requires extensive training standards that are hard to regulate [13].

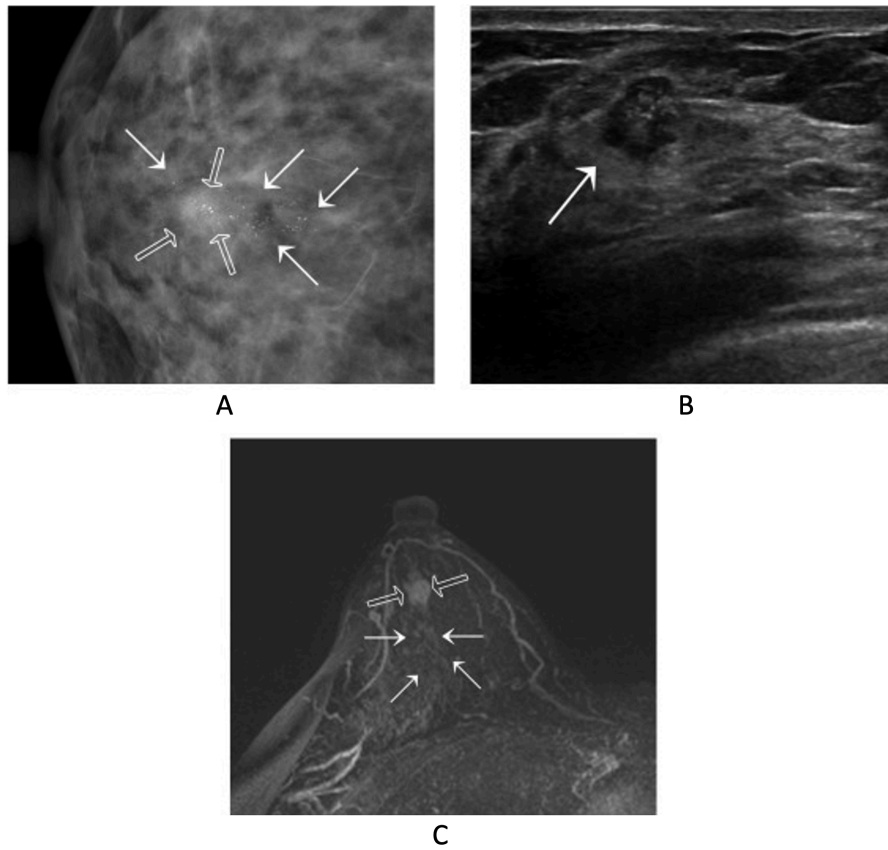


Figure 2: Images of an approximately 40mm invasive breast cancer. A - Mammography, B - Ultrasound, C - Magnetic Resonance Imaging. Retrieved from [2].

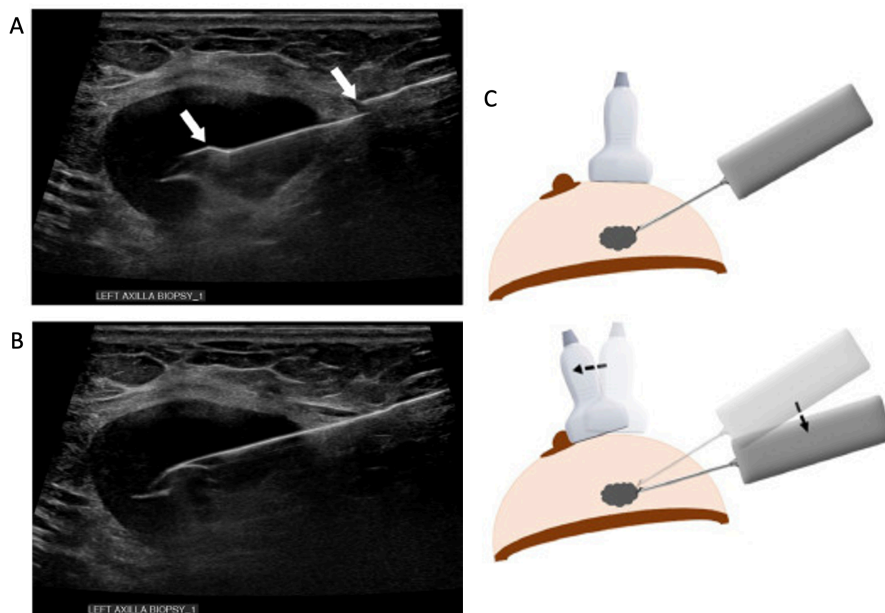


Figure 3: A and B - Ultrasound imaging of the needle obtaining a sample. C - Breast biopsy procedure representation. Retrieved from [3].

1.3 OncoNavigator Project

The OncoNavigator project, which this dissertation integrates, aims to improve the precision of the current breast cancer interventions by combining information from real-time medical imaging with a collaborative medical robot. It also aims to integrate novel visualization techniques with device tracking to enhance medical training. This project is a part of 2Ai, a research-based organization within the Polytechnic Institute of Cavado and Ave (IPCA).

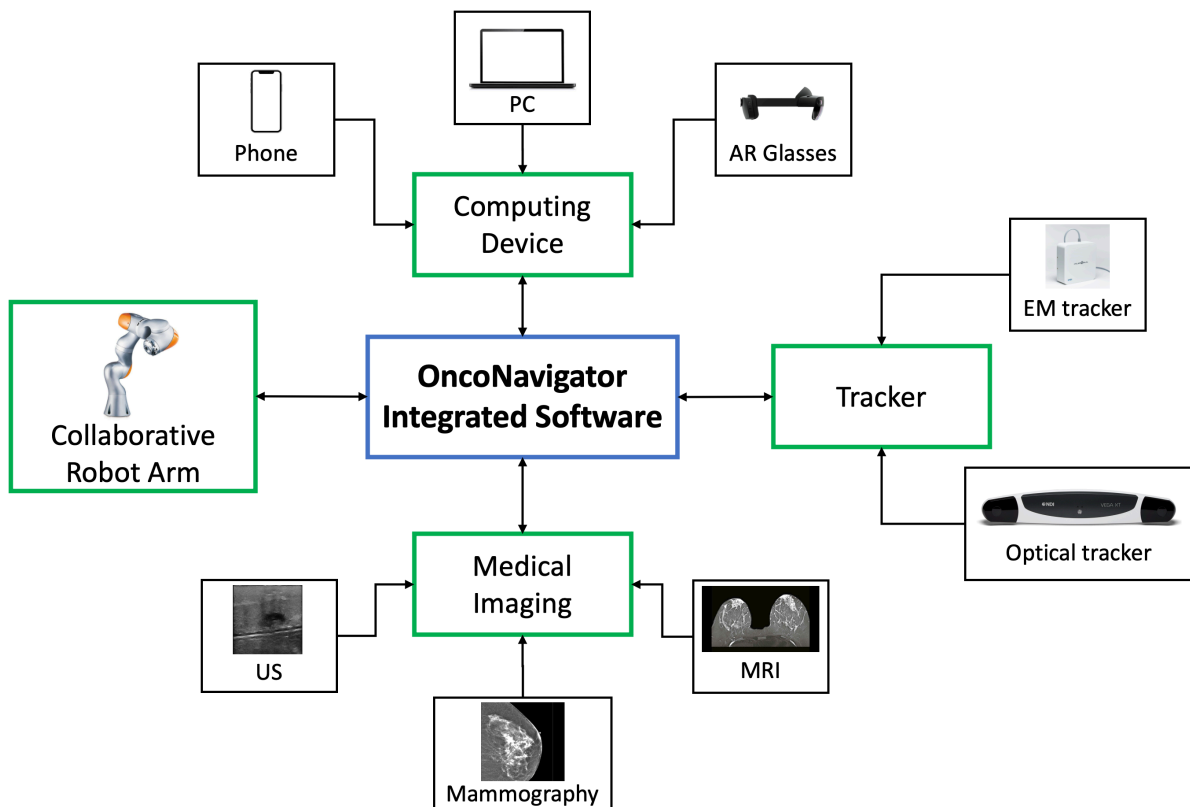


Figure 4: OncoNavigator project overview.

The OncoNavigator framework aims to increase the efficiency of traditional breast oncological procedures by adding the required precision of robot-guided systems, and by increasing the intra-interventional information with enhanced lesion visualization. The framework aims to lower human error, lessen the influence of physician expertise, and improve patient procedure outcomes.

The development of the OncoNavigator navigation framework will follow a modular approach. The system will be composed of independent modules ranging from robotic communication modules to electromagnetic tracker interaction modules to portable US probe real-time image input modules. Figure 4 shows all of the planned modules of the project.

The modular approach methodology allows for greater independence between modules, potentially

making the system more stable and upgradeable. This approach increases the stability of the solution because it allows system recovery by reactivating or even fixing a single failing module, making the overall system more resilient. Upgradability occurs as a side-effect of the modular approach, for example, if a new US probe is released into the market and the system administrators want to add it to the solution, a new module would be developed for it and few changes would need to be done in the main framework to include it. This characteristic is vital to a framework like this since it combines different technologies, and maintaining it up-to-date is important to improve or add features.

The project is large and is therefore composed of a multidisciplinary team from different areas. The main areas of interest for this dissertation are medical navigation systems and their underlying software, along with robot-assisted breast biopsy systems and robot communication protocols. Thus, a research effort was made into the state of the art of these areas which is described in the next sections.

1.4 Medical Navigation Systems

The rise of imaging technology has transformed medical treatments in the past decades by becoming less invasive and more accurate. They compose navigated interventions of image guidance and real-time position tracking. This raises the need for software platforms that integrate both aspects [14].

Image Guided Therapy refers to minimally invasive methods in which the operator relies heavily on images to guide the intervention. These operations require highly precise and up-to-date imaging methods. The following are some software platforms/libraries that have been facilitating Image-Guided therapy.

The Image Guided Surgery Toolkit is an open-source library designed for the prototyping and development of image-guided surgery applications. This library implements an abstraction layer that facilitates the incorporation of different tracking devices. This library, however, is no longer being updated, having received its last update in 2013.

The Medical Imaging Toolkit is an open-source cross-platform library designed for the development of interactive medical image processing software [15]. This library is extensible and modular, and because of this, several open-source extensions have popped up, like the Medical Imaging Toolkit for Image-Guided Therapy [16]. The software enables communication with some tracking hardware, such as optical or electromagnetic tracking devices; processing data tracking, through a navigation pipeline, and rapidly prototyping navigation applications [17].

3D Slicer is a free, open-source, and cross-platform software for the visualization and analysis of medical image datasets. It has support for multi-modality imaging, including MRI, computerized tomography,

US, nuclear medicine, and microscopy [18]. Image-guided and navigated interventions are supported by an extension called SlicerIGT. This extension includes a set of modules for recurring tasks in interventions, as well as tools that allow software developers to design customized Graphical User Interface (GUI) for intraoperative usage [14].

CustusX is a free and open-source software that combines images, surgical instrument tracking, and a computer display, in order to create a complete navigation system. It contains a toolbox of navigation features, image-processing algorithms, connections to external hardware and other useful tools for Image-Guided Therapy [19].

1.5 Robot Assisted Breast Biopsy

Robots can help in invasive medical procedures; this is especially true when imaging methods are also involved in the procedure. A target or a path can be defined (as an image) and then, an algorithm can plan the route and position the robot accordingly. These systems can even compensate for organ repositioning during the procedure caused by breathing or patient movement and are not subjected to human afflictions [20].

One of the first systems for robot-assisted US-guided biopsy was developed by Megali *et al.* [21]. The developed system comprised a robotic arm that handles the biopsy needle, a US scanner, a tracking system, and a computing device, which presents the GUI. It works by placing the biopsy needle at the end effector of the robot arm. The physician then selects the desired target within the US image and the robot arm subsequently places the needle along the correct path.

More recently, Abayazid *et al.* [22] presented a system capable of automatically steering a biopsy needle under US guidance. It works by performing an US pre-operative scan for three-dimensional lesion localization and breast shape reconstruction. The system, whilst being sufficiently accurate for targeting lesions of at least 3mm in radius, is not dynamic. This implies that it cannot account for the patient's movements without doing another scan.

1.6 Robot Communication Protocols

Image-Guided interventions require several systems to communicate reliably and quickly, so communication protocols designed for this purpose were developed on top of the transport layer.

The transportation layer handles communication between systems on the Internet Protocol (IP) stack. Transportation layer protocols provide various features, such as congestion control, reliability, in-sequence

delivery, and flow control that contribute to the performance and quality offered by the communication network. Of all transport layer protocols, the most used are Transmission Control Protocol (TCP) and User Datagram Protocol (UDP) [23] [24].

TCP is a tried-and-true transport layer protocol that offers a variety of benefits such as reliability, flow control, and congestion control. TCP can transfer a continuous stream of data between systems, it also can recover data damaged, lost, or duplicated over the network. It also provides a mechanism that helps the receiver control the amount of data sent by the sender, and provides a congestion avoidance mechanism to reduce the transmission rate when the network becomes overloaded [25].

UDP is a transport layer protocol that does not guarantee any reliability or in-order delivery of data packets. A UDP packet, is divided into two parts, a header, and the data itself, it also employs a cyclic redundancy check to inspect for the integrity of packets. If an error is found the mechanism simply discards the packet, and doesn't attempt to recover it [26].

TCP is very desirable in most applications, however, it comes at the cost of being slower and using more network bandwidth than UDP (Figure 5). UDP is considered where the in-time delivery of data is important rather than a reliable ordered delivery, such as voice and video traffic [27].

One of these protocols is OpenIGTLink, which is an open-source and cross-platform network communication interface, made on top of the communication layer, specifically designed for image-guided interventions. It aims to provide plug-and-play unified real-time communications in operating rooms for image-guided interventions, where imagers, sensors, surgical robots, and computers from different vendors need to work cooperatively, by defining data packages for all kinds of devices used in medical interventions [28].

OpenIGTLink is used in a variety of other medical libraries, such as PLUS, which is a software toolkit for data acquisition, pre-processing, and calibration for navigated image-guided interventions [29]. This toolkit uses OpenIGTLink to retrieve data from surgical navigation systems, positioning devices, or USB cameras. The robot building software toolkit robot operating system has an extension called ROS-IGTL-Bridge that enables cross-platform data sharing between the robot operating system and medical image computing software using OpenIGTLink [30]. The abovementioned SlicerIGT also uses OpenIGTLink to communicate with hardware devices.

Another protocol developed for Image-Guided Therapy communications is the Computer-Aided Medical Procedures Communication which is a generic, cross-platform, portable, lightweight, and easily extensible, client-server-based framework, that can control the communication between multiple imaging and tracking devices. It shows similar performance to OpenIGTLink while offering additional features, such as

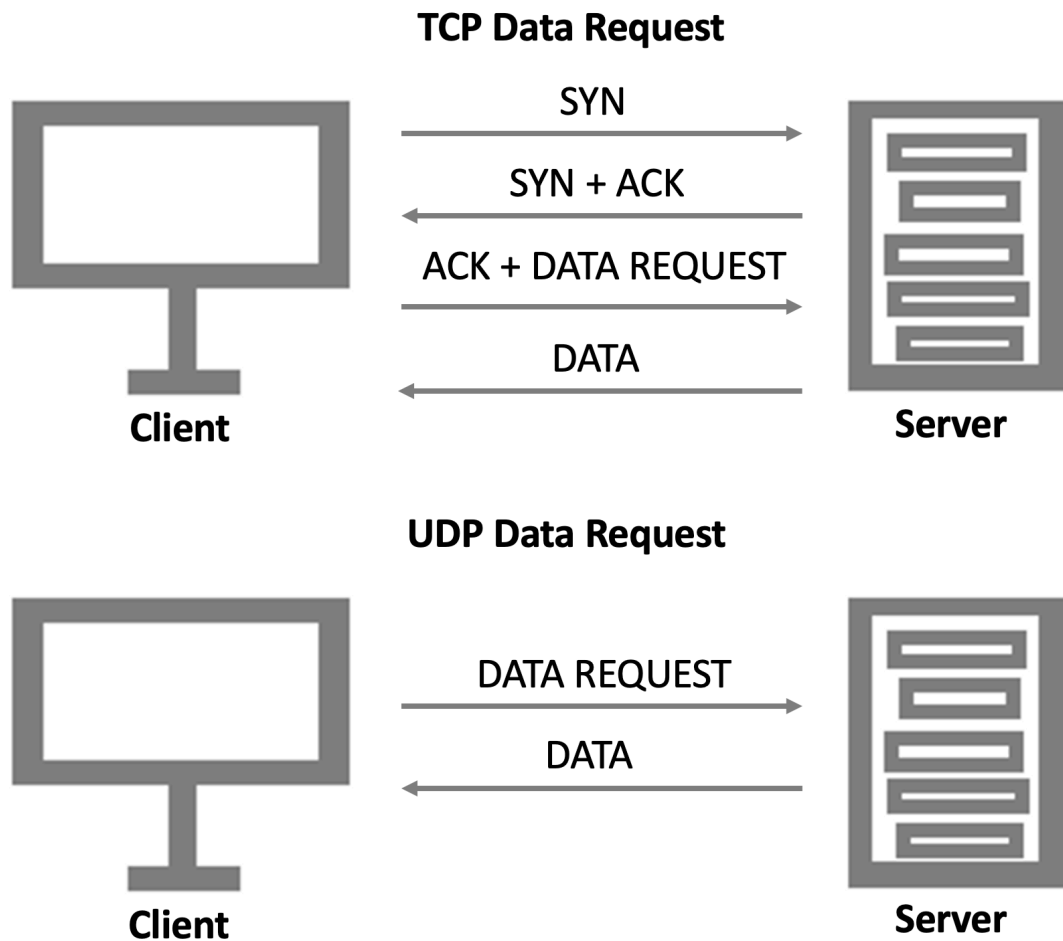


Figure 5: TCP and UDP workflows.

prioritization in communication and data compression, to reduce bandwidth [31].

1.7 Motivation

The OncoNavigator project consists of integrating a collaborative medical robot with medical imaging along with the use of Augmented Reality (AR) devices for medical training, having in mind the following goals: Breast cancer lesions need to be detected as soon as possible and the screening process needs to become more efficient to meet the needs of an ever-growing demand for medical care. Since US-guided biopsy heavily relies on the operator's expertise, this project allows medical students and doctors to experience the procedure with robotic aid or AR enhancing their abilities.

1.8 Research Questions

In the development of this dissertation the following questions will be answered:

1. Can AR glasses be an effective tracking option in a medical context?
2. Is it possible to develop an effective training solution using AR glasses for the US-guided breast biopsy procedure?
3. Can automatic breast lesion segmentation be incorporated into real-time US imaging?

1.9 Objectives

The main objective of this dissertation is to improve the precision of current breast cancer interventions within the OncoNavigator framework. As already described, the framework is composed of a set of independent modules (defined according to the requirement of the OncoNavigator project) that communicate, in a controlled way, with a central unit. To demonstrate the potential of this modular framework two specific use cases were defined and implemented. These use cases were later evaluated in a laboratory environment to correctly evaluate the performance (both technical and functional) of the proposed framework.

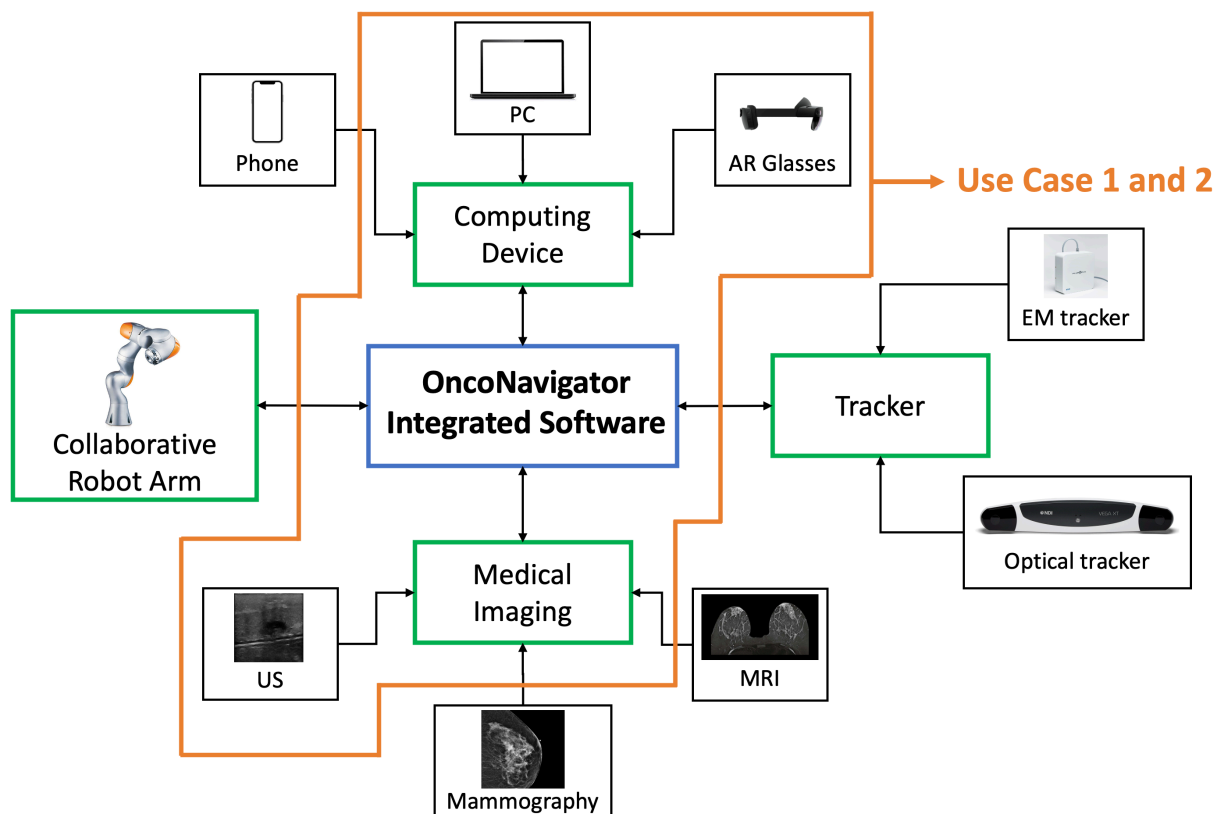


Figure 6: Use case 1 and 2 compared with the overarching OncoNavigator framework.

Use cases 1 and 2 (Figure 6) focus on the usage of AR glasses in displaying US imaging. Use case 1 employs the HoloLens 2 AR glasses to track the movements of an US probe. It utilizes the attained tracking

information to generate an US image from a 3D US blob. The probe's movements were tracked with the HoloLens 2 camera. A QR code mounted on the US probe was the camera's image target. A paper was produced based on this use case, entitled "Ultrasound training simulator using augmented reality glasses: an accuracy and precision assessment study". This paper was published at the 44th Annual International Conference of the IEEE Engineering in Medicine Biology Society (EMBC) and presented as a poster from the 11th to the 15th of July 2022. This work is presented in its entirety in chapter 2.

The second use case consists of an enhancement proposal for breast biopsy procedures using the HoloLens 2 AR glasses as a visualization tool. It used the results presented in the first use case, which relied on QR code tracking. Real-time US imaging with lesion segmentation is displayed in the AR environment along with needle trajectory. This research was described in a paper entitled "Augmented reality-assisted ultrasound breast biopsy" and will be submitted to an international journal. This paper is presented in its entirety in chapter 3.

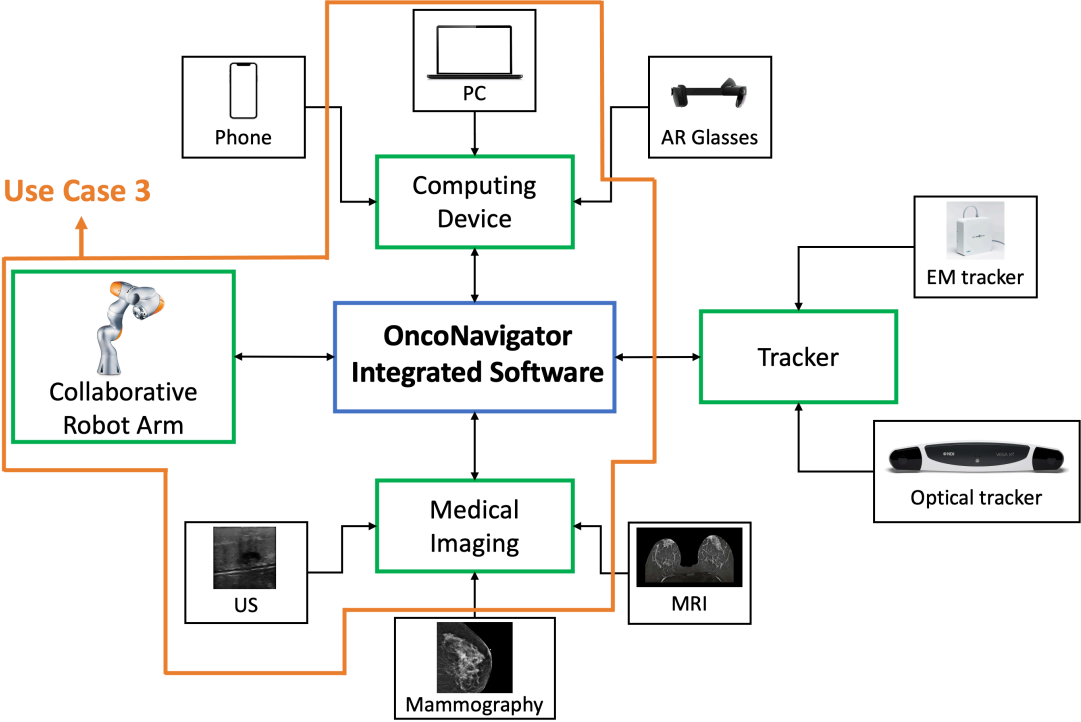


Figure 7: Use case 3 compared with the overarching OncoNavigator framework.

Use case 3 (Figure 7) consists of a proof-of-concept software used in a robotized breast biopsy procedure. It controls a robot arm mounted with an end-effector that houses a portable US probe. The software displays real-time US imaging from the portable probe overlaid with a convolutional neural network lesion segmentation. A trajectory from the biopsy needle is also displayed so it can help the user in the procedure. This software is presented in chapter 4.

1.10 Dissertation Structure

This work is divided into five chapters. This chapter presents the dissertation's context and objectives. Chapter 2 is composed of the adaptation of a scientific paper entitled "Ultrasound training simulator using augmented reality glasses: an accuracy and precision assessment study" submitted to an international peer-reviewed conference. Likewise, a scientific paper, yet to be submitted, is characterized in chapter 3, entitled "Augmented reality-assisted ultrasound breast biopsy".

Chapter 4 goes in-depth on a developed US software for the enhancement of real-time breast interventions with US imaging. Finally, chapter 5 is dedicated to expressing conclusive thoughts and future work.

Chapter 2

Ultrasound training simulator using augmented reality glasses: an accuracy and precision assessment study

This chapter has been published at an international conference: **José N. Costa**, João Gomes-Fonseca, Simão Valente, Luís Ferreira, Bruno Oliveira, Helena R. Torres, Pedro Morais, Victor Alves, João L. Vilaça, "Ultrasound training simulator using augmented reality glasses: an accuracy and precision assessment study", in 2022 44th Annual International Conference of the IEEE Engineering in Medicine & Biology Society (EMBC). <https://doi.org/10.1109/EMBC48229.2022.9871406>

The paper describes the development of an ultrasound training simulator in an augmented-reality system along with the validation of the aforementioned system's tracking precision.

Minor adaptations to the original publication have been performed. The figures and section numbers were updated with the chapter title and all references were combined in a common final section.

Abstract

US imaging despite being safe, cost-effective, and radiation-free, presents poor quality and artifacts, requiring specific medical training in US probe handling and image evaluation. The use of simulators to train physicians has proven its effectiveness, but most of them require specific facilities and hardware. In the last few years, AR has gained relevance to simulate real scenarios which can avoid large setups and broaden medical training to more physicians. This work proposes a new framework for the training of US images acquisition. It consists of a custom-made application that runs on AR glasses (Microsoft HoloLens 2) and interacts with a US simulator application. The AR glasses track the orientation of a QR code mounted on a US probe, communicating its orientation with the US simulator application. This allows the physician to interact with a US probe seeing in real-time the US image in the physician's field of view. The QR code tracking assessment of the AR glasses was conducted by measuring the orientation accuracy and precision when compared with the measures of an electromagnetic tracking device (i.e., NDI Aurora). The proposed solution presented a good performance, rendering the US image in AR glasses with real-time feedback. Moreover, it can track the QR code on the US probe with an accuracy of 0.755° , and a precision of 0.018° . Overall, the proposed framework presents promising results and the use of AR glasses as a tracking device reached a good performance.

Clinical Relevance– Simulation is a relevant tool to train physicians, especially in US imaging. AR glasses can broaden the training to less trained physicians by reducing the need for complex setups. This technology allows the implementation of a more natural user interface, which can be relevant in scenarios where good coordination between the eyes and hands of the physician is necessary (i.e., Biopsies).

2.1 Introduction

Smaller and less costly US equipment has been leading to the growth of the usage of ultrasonography by medical specialties. Although US imaging has historically been seen to be harmless, its use is heavily reliant on the operator [32]. This is owing to the poor image quality and artifacts, such as speckle noise, shadows, or signal dropout, which limits interpretation and may mislead diagnosis. As a result, there has been an upsurge in research of US simulators for medical training in recent years [33].

Some US simulators give the user a realistic experience as well as personalized training activities, they rely on large and fixed hardware [34], [35]. Other approaches rely on a personal computer (PC), manufacturer-supplied software, a USB probe and customized training [36], [37]. Web-based solutions are also available where the user does not need to download or install any additional software and can

use the PC mouse to change the rotation of a virtual probe [38]. Some of these systems also allow for the integration of a smartphone, allowing for the simulation of the probe's movement using data from the smartphone's sensors [39]. However, the need for a secondary screen makes the whole process less intuitive, since the user needs to be constantly alternating his attention between the probe's movement and the screen output.

The previous limitation can be mitigated with the use of AR imaging systems. These systems work by layering virtual information over a real image [40]. Moreover, an AR system can also track the movements of objects using cameras and display the information over them, eliminating the need for the user to shift the attention from the object's movements [41]. AR techniques for US navigation employing head-mounted displays were first developed decades ago [42], [43].

This paper describes the integration of the HoloLens 2 [44] AR glasses with the US simulator developed by our team in [33]. Moreover, it measures the accuracy and precision of AR Glasses on tracking the US probe movements compared to an Electromagnetic Tracking (EMT) system.

This work is structured as follows. In Section 2.2, we present how the proposed framework was developed. In Section 2.3, the experiments made to validate the accuracy and precision are presented. In Section 2.4, we present the results acquired from the experiments conducted. In Section 2.5 and 2.6, we discuss the results and present the main conclusions.

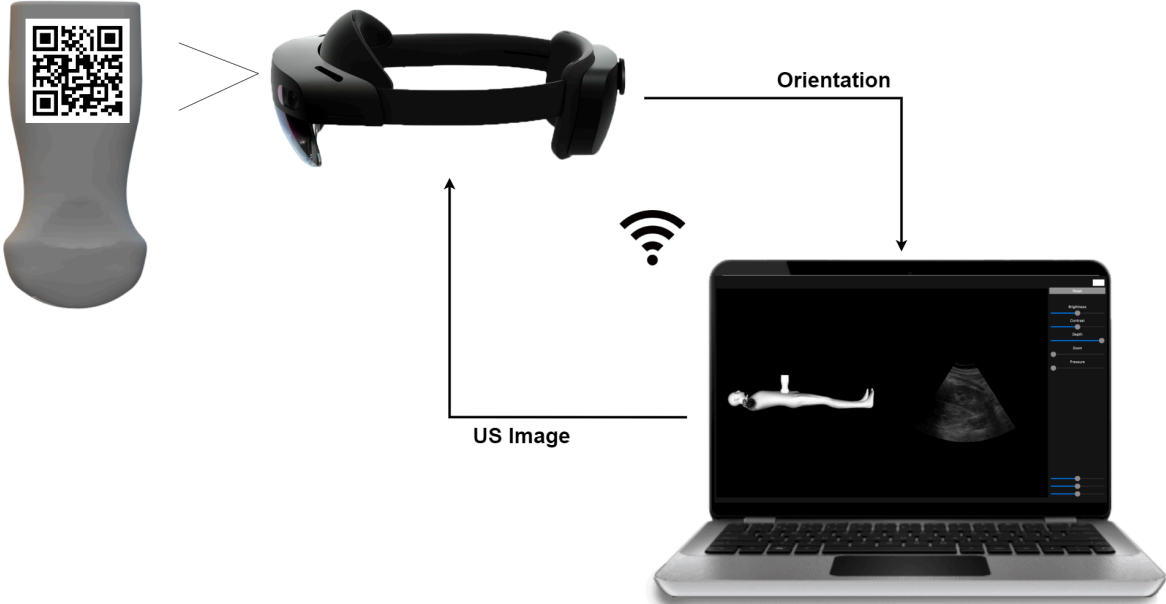


Figure 8: Overview of the proposed framework.

2.2 Methods and Techniques

2.2.1 Overview

The proposed solution uses a modified version of the US simulator developed in [33], HoloLens 2 AR glasses, and a portable US probe [45] with a 7 cm wide QR code.

The system basis relies on the estimation of the position/pose of a QR code. The QR code is tracked by the glasses and its position/orientation transmitted to the US simulator application via a Wi-Fi connection. The application proceeds to slice a template 3D volume with the input orientation, and the resulting 2D US image is sent back to the HoloLens glasses. The framework is presented in Figure 8.



Figure 9: View from HoloLens display showing the US image over the QR code assembled at the top of the portable US probe.

2.2.2 QR Code Tracking

The QR Code tracking module for HoloLens 2 was developed in C# using Unity 3D 2020 [46] (version 2020.3.25f1), Microsoft's Mixed Reality Toolkit for Unity [47], Visual Studio 2019 [48], Vuforia AR Software Development Kit (SDK) [49].

The HoloLens video feed was passed as an input to the Vuforia SDK to detect the QR code image in 3D space. Vuforia needs prior knowledge of the QR code image and its real-world size. Vuforia tracks images by looking for QR code features on an image [50].

The US probe was fitted with a 3D printed case that allows the QR code to be assembled to it (Figure 9). Once the pattern is identified, the holographic image is placed on top of the QR code and shows the US image whenever is available. The QR code tracking provides data consisting of Cartesian coordinates (x , y , and z) and quaternions (q_0 , q_x , q_y , and q_z).

2.2.3 US Simulator

As abovementioned, the US simulator developed by Valente *et al.* [33] was used and adapted in this work.

This strategy uses an offline 3D US volume that is sliced according to the movements registered on an instrumented probe. Since the original version only supports orientation modification, always keeping the probe's position in the center of the volume, our entire framework was adapted to only work with orientation parameters. Therefore, the US simulator receives orientation data (i.e., quaternions) from the QR Code tracking system. This data is then used to slice a template 3D volume, resulting in a 2D US image. After, the image is sent to the HoloLens 2 application displaying it over the QR code. Two separate threads were added to the US simulator application to handle the received and sent data. This was necessary to achieve a real-time application response.

Before using the US simulator, a calibration is required. Thus, the calibration of the probe's orientation is done using the same strategy presented in [33], consisting of defining a new orientation reference. A reset button is used to save a quaternion that will be used as reference during the simulation.

2.2.4 Communication

To connect the HoloLens 2 application with the US simulator application, the system requires a network connection. A TCP/IP connection (AR glasses as a server) was used to send the QR code pose to the US simulator application every time a frame is rendered. Once a TCP/IP connection is established between the two applications, the US simulator also starts streaming US images at a rate of around 35 Frames per

Second (FPS) through UDP packets.

Thus, the US image's data is divided into multiple UDP packets. A custom UDP packet was made to send the data, which includes an 18-byte header with information about the packet number being sent as well as a timestamp value for every different US image. Note that this information allows the application to check whether or not a packet was lost on the network.

2.3 Experiments

2.3.1 Experimental Setup

A scaffold (a spherical structure with hexagonal holes) was 3D printed in polylactic acid material using an Ultimaker II Plus [51]. The printer uses the fused deposition modeling technique, with a printing resolution 0.2 mm. The scaffold was used to rigidly fix the probe at specific orientations.

Besides, an acrylic platform was specifically designed to perform the experiments. The whole acrylic glass platform was projected on a CAD software [52] and cut on a laser cutting machine [53] with a cutting precision of ± 0.04 mm. The acrylic platform enables positioning the scaffold at the center of the field generator volume, where the accuracy and precision are superior.

The 3D printed case used to attach the QR code was also designed to place the EMT sensor within it, the sensor was placed behind the QR code to improve the consistency of accuracy and precision assessment.

2.3.2 Orientation Accuracy and Precision

To measure the orientation accuracy and precision of the QR code tracking based on HoloLens 2, the probe was placed on the scaffold and compared against a commercially available EMT system, i.e. the NDI Aurora [54]. The Planar Field Generator and the 6DOF Reference sensor was used during experiments. As abovementioned, the EMT sensor was attached to the probe using the same 3D printed case where the QR code was attached.

A custom software application was developed using MATLAB [55] (version R2018a) to acquire the orientation of the EMT sensor and QR code tracking. For each orientation, 10 samples were recorded for both systems.

As shown in Figure 10, six different positions were assessed in the scaffold with each position being measured five times. Position 1 was used to measure the accuracy along probe's central axis where

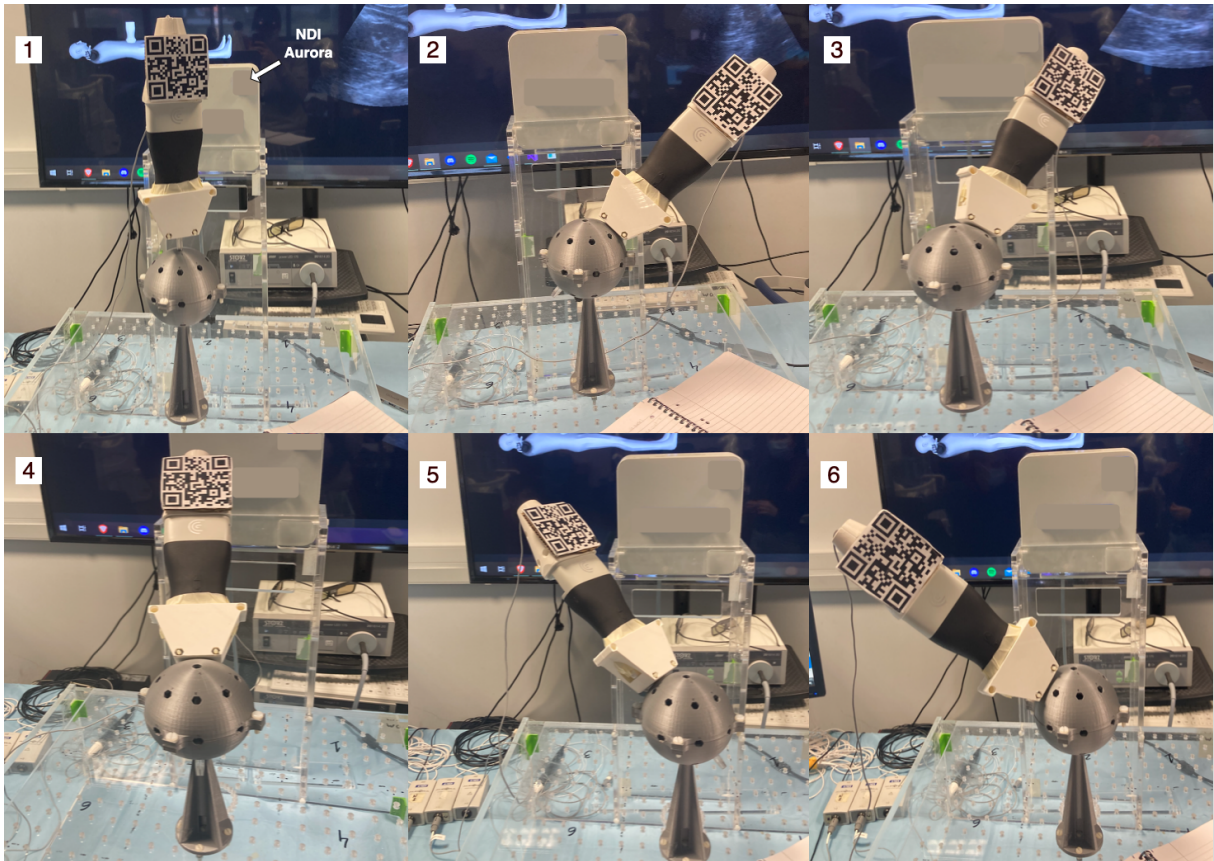


Figure 10: The 6 different orientations tested during accuracy and precision assessment.

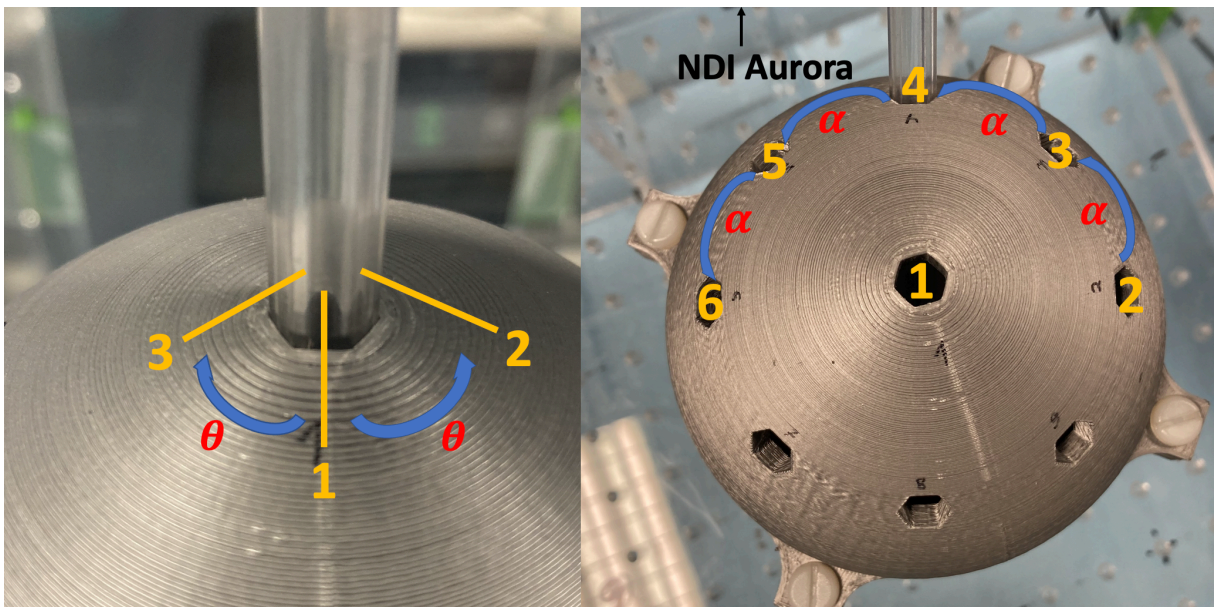


Figure 11: Measured rotation along the probe's central axis represented by θ on the left. Movements used to calculate accuracy represented by α on the right.

differences between 3 orientations were measured. The scaffold configuration differences must be 60° between consecutive orientations which are represented here by θ . The same process was repeated for

the other positions, and the differences were measured. Herein, the scaffold configuration presents 45° between consecutive orientations which are represented by α . Figure 11 shows measurements detailly. The orientation accuracy and precision were calculated according to Gomes-Fonseca *et al.* [56].

2.4 Results

2.4.1 Orientation Accuracy and Precision

Table 2 shows that the accuracy of the HoloLens 2 and the NDI Aurora systems are close, achieving results near to the ground-truth orientation. On average, the NDI Aurora system has an accuracy of 0.775° and the HoloLens 2 system 0.755° . Particularly, the angle measured between 3 and 4 shows the largest difference to the ground truth in both systems.

Table 2: Orientation accuracy measured between different positions (Mean \pm Standard Deviation).

Position differences	Accuracy		
	Ground-Truth	NDI Aurora	HoloLens
α_{2-3}	45°	$44.64^\circ \pm 0.16^\circ$	$44.6^\circ \pm 1.00^\circ$
α_{3-4}	45°	$43.54^\circ \pm 0.07^\circ$	$42.63^\circ \pm 0.66^\circ$
α_{4-5}	45°	$44.14^\circ \pm 0.44^\circ$	$44.39^\circ \pm 0.56^\circ$
α_{5-6}	45°	$44.09^\circ \pm 0.86^\circ$	$44.28^\circ \pm 1.20^\circ$
θ_{1-2}	60°	$60.55^\circ \pm 0.21^\circ$	$59.79^\circ \pm 0.26^\circ$
θ_{1-3}	60°	$60.51^\circ \pm 0.14^\circ$	$60.22^\circ \pm 0.12^\circ$

Table 3 shows that the precision of both systems is similar, with an average of 0.0094° in the NDI Aurora and 0.0180° in the HoloLens 2 system.

Table 3: Orientation precision measured at each position (Mean \pm Standard Deviation).

Precision	
NDI Aurora	HoloLens
$0.0094^\circ \pm 0.0063^\circ$	$0.0180^\circ \pm 0.0217^\circ$

2.5 Discussion

In this paper, we describe and technically evaluate a solution for US training, which consists of the HoloLens 2 AR glasses that by tracking the orientation of a QR code mounted on a physical probe-sized object, can communicate the captured orientations, via wireless communication, with a US simulator application developed in [33]. This application uses the received orientation to slice a 3D volume to generate a 2D US image. Overall, the process of sending the probe's orientation, processing the orientation, receiving the US image, and loading the US image runs at 35 frames per second.

According to the literature, a similar solution to the proposed in this work was presented in [41]. However, this solution is not meant to be for US medical training, since it only has the purpose of showing a live output of a real US probe. To the best of our knowledge, no study has offered a method that employs AR glasses to concurrently acquire the orientation of a US probe and show the resulting US picture, which is required to avoid the user diverting their attention away from the probe's movement. 2

The results show that the HoloLens system is capable of accurately and precisely capture orientation data when compared against a high precision EM tracking system. Indeed, the HoloLens 2 were consistent with those measured in [56] for EM systems. It was observed a larger difference between $\alpha_3 - 4$ (Table 2) on both systems, which can be related to slight errors in the manufacturing of the scaffold.

As for future work, the HoloLens 2 computational capabilities should be leveraged to compute the 2D slice, instead of relying on an external application to do this. At the moment only the probe's orientation is being tracked. In the future, the possibility of tracking the probe's position is also envisioned. Thus, a better interaction with the system is expected since the probe doesn't need to be in a fixed position. A different approach to tracking without QR codes will also be studied to simplify the system. A comprehensive tutorial will also be attempted, to help new trainees improve their practices without supervision. Clinical validation will also be pursued.

2.6 Conclusion

This work presents an AR US simulator to potentially accelerate and facilitate the learning curve of physicians in handling and interpreting US images. The prototype solution proved the concept and showed that QR code tracking is accurate and precise, demonstrating potential use for medical training. Further clinical validation is missing.

Chapter 3

Augmented reality-assisted ultrasound breast biopsy

This chapter will be submitted in an international conference or journal: **José N. Costa**, Luís Ferreira, Augusto R. V. F. de Araújo, Bruno Oliveira, Helena R. Torres, Pedro Morais, Victor Alves, João L. Vilaça, "Augmented reality-assisted ultrasound breast biopsy".

The paper describes the development of a breast biopsy augmented reality system, along with a comparison with the traditional breast biopsy procedure and system latency assessment.

Minor changes to the original publication have been performed. The figures and section numbers were updated with the chapter title and all references were combined in a common final section.

Abstract

Breast cancer is the most prevalent cancer in the world, excluding nonmelanoma skin cancers, and the fifth-leading cause of cancer-related death. It is well known that treatment is most effective in its early stages. Thus, a need to screen considerable portions of the population is crucial. When the screening procedure uncovers a suspect lesion, a biopsy is performed to assess its potential for malignancy. This procedure is usually performed using real-time US imaging. In recent times, AR has become more relevant in medical applications. Displaying data in the user's field of view may improve visualization and aid diagnostics analysis. This work proposes a visualization system for US breast biopsy. It consists of an application running on AR glasses (Microsoft HoloLens 2) that interacts with a companion computer application. The AR glasses track the position of QR codes mounted on an US probe and a biopsy needle. Then, US images are shown in the user's field of view along with enhanced lesion visualization (segmented through a convolutional neural network) and biopsy needle trajectory. To validate this system, the latency of the transmission of US images was evaluated. Moreover, a usability assessment compared our proposed prototype with a traditional approach with different users. It showed the needle alignment became more precise, with $92.67 \pm 2.32^\circ$ in our prototype versus $89.99 \pm 37.49^\circ$ in a traditional system. The users also reached the lesion more accurately. Overall, the proposed solution presents promising results, and the use of AR glasses as a tracking and visualization device exhibited good performance.

Clinical Relevance– AR allows the implementation of an immersive user interface, which can be relevant in scenarios where hand-eye coordination is paramount for physicians, such as biopsies. This system can also allow real-time streaming of a particular procedure, potentially allowing collaboration and co-decision.

Keywords– Ultrasound, Breast Biopsy, Augmented Reality, Convolutional Neural Networks, Lesion Segmentation.

3.1 Introduction

The leading cause of death worldwide is cancer [7]. Breast cancer is the world's most prevalent cancer, excluding nonmelanoma skin cancers, and the fifth leading cause of cancer death, with 2.3 million women diagnosed and 685,000 deaths worldwide in 2020 [57]. Though a sizeable portion of breast cancer cases does not result in death, they significantly reduce the quality of life and generally come with higher expenses.

The treatment of this type of cancer is more effective in its early stages. As a result, medical imaging modalities such as MG and US have been used to screen substantial parts of the population [8], [10]. When MG or US finds a suspicious lesion, a biopsy is performed to evaluate the nature of the assumed lesion. A biopsy consists in taking a small sample of body tissue so it can be examined in a laboratory to determine its potential for malignancy. Currently, real-time US-guided biopsy is the preferred method to perform a breast biopsy [12].

US imaging is a non-invasive, radiation-free technique that effectively captures tissue characteristics by transmitting sound waves into the body and recording the waves that echo back to construct an image. It requires relatively simple technology and has no known harmful effects on health. In US, since the image is dynamically acquired and relies on the 3D motion of the probe, operator expertise is critical during acquisition; poor image quality and eventual artifacts further increase the demand on the operator's expertise [58]. In conventional clinical practice, lesion identification in US is purely based on images through a naked-eye evaluation. Contouring lesions can be performed to extract relevant information, but it takes time and depends on the observers [59]. As a result, several methods have been suggested for an automatic lesion segmentation. Active contour, region-growth, and threshold-based techniques were the main segmentation techniques used in early research. These techniques, however, frequently require manual intervention [1]. Recently Convolutional Neural Networks (CNN) have surpassed traditional image processing techniques and are showing promising results in breast US segmentation [60], [61].

Subpar quality in US imaging can cause the performing physician to miss the lesion [62]. Furthermore, the sampling of lesion tissue can also have a maximum error rate of 10%, according to J. Heil *et al.* [63]. The biopsy procedure is, therefore, highly dependent on the skills of the physician. This work aims to improve this procedure by utilizing CNN lesion segmentation to help analyzing US images and by incorporating AR, that provides relevant information, such as the real-time tracking of the biopsy needle, in the field of view.

AR-based imaging systems may be helpful in the biopsy procedure. Essentially, these systems work

by superimposing digital data over the user's field of view (captured by the camera), creating the illusion that holographic content is a part of the real world. They can also utilize cameras to track the movements of objects and display information along those movements, removing the need for the user to look away from the object's motion [40].

The integration of US-guided breast biopsy with AR systems was initially attempted in 1996 by Fuchs *et al.* [42]. In this initial work, the results were promising, and the developed system was sufficiently robust and accurate. Feedback from physicians reported that it helped the procedure; however, it had a lengthy setup process and no needle guidance. Due to technological limitations, the AR device weighed nearly six pounds. That work was continued by Rosenthal *et al.* [64] in 2002. They used more advanced AR glasses and implemented needle trajectory. More recently, in 2020, Asgar-Deen *et al.* [65] compared the usage of AR to a traditional monitor in a simple stationary breast biopsy procedure. In 2021 Gouveia *et al.* [66] utilized AR in magnetic resonance-assisted breast cancer surgery, and in 2022, Kashiwagi *et al.* [67] and Nguyen *et al.* [41] experimented with AR glasses as a visualization tool for US images. These solutions only display the US images in the user's field of view. Our solution places the US image with lesion location information in the correct position according to the real position and orientation of the US probe.

The objective of this work is to conceive a solution to train or increase the efficiency of physicians with the US-guided breast biopsy procedure. This paper describes a system prototype that utilizes the HoloLens 2 [44] AR glasses for the enhancement of the US-guided breast biopsy procedure. It combines real-time US video, CNN segmentation, and object tracking to provide an enhanced visualization of the procedure. Moreover, the system's latency is measured by comparing the developed system with an optical tracking device and the usability assessment of different users. It is structured as follows. Section 3.2 presents how the proposed system was developed, followed by Section 3.3, which explains the experiments to assess usability and latency. The data gathered from the experiments is presented in Section 3.4, and Section 3.5 discusses the achieved results. Finally, Section 3.6 presents the main conclusions.

3.2 Methods and Techniques

3.2.1 Overview

The developed prototype uses a portable US probe, more specifically the Clarius L15 HD Portable Handheld Scanner [45], an automatic biopsy needle [68], the HoloLens 2 glasses, a computer, and two 7 cm wide QR codes mounted on 3D printed cases (Figure 12). The system is divided into an application running in

AR glasses and a computer application.

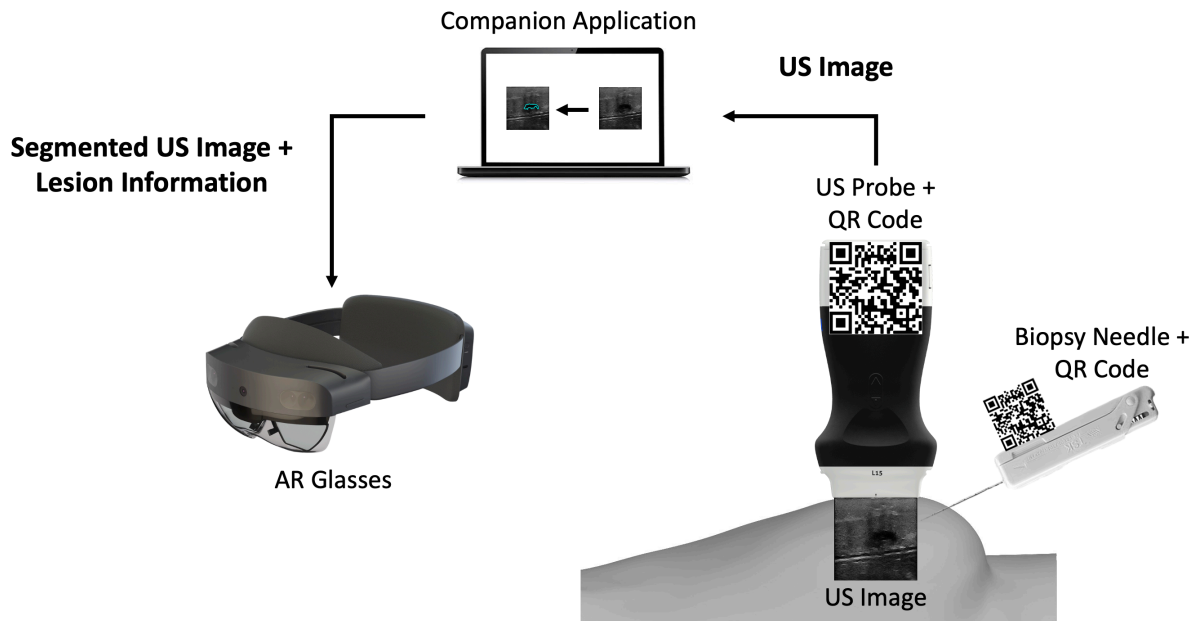


Figure 12: Overview of the different components of the proposed prototype.

The computer application is a companion to the AR application. It works by: i) connecting to the US probe; ii) processing the real-time incoming US images by segmenting them through a CNN network, and iii) sending those images to the AR application afterwards.

The AR application running on the glasses is mainly a visualization tool. It tracks two QR code tags mounted on the US probe and the biopsy needle, so it can perform real-time tracking of both. It displays in the user's field of view the real-time US video stream along with a trajectory from the needle tip to the lesion and validates its orientation.

3.2.2 Companion Application

The necessity for real-time US imaging is crucial in the biopsy procedure. However, US imaging presents poor quality and requires a high level of expertise to be interpreted [32]. In light of this, the solution must show real-time US video and provide a more straightforward US imaging interpretation.

Incompatibilities and limitations with the AR glasses system led to the development of a computer application that feeds data to the AR application. This data consists of the real-time streaming of US video from the US probe's Application Programming Interface (API) along with the CNN lesion segmentation data. The CNN segmentation required an NVIDIA [69] Graphical Processing Unit (GPU) since it relied on its CUDA API [70], [71]. Since the AR system was lacking such a GPU, this computation had to be

performed on a computer. The abovementioned CUDA API makes use of the parallelism available in a GPU to speed up computations [72], [73], such as CNN operations [74]. This application was developed using Qt [75] (version 5.15), to create the GUI, and OpenCV [76] (version 4.5.5) was utilized to do US image processing and lesion segmentation.

US Breast Lesion Segmentation

The workflow of the companion application starts with the reception of a new US image frame from the US probe. This image has 512x512 pixels, dimensions manually set in the probe's API. These dimensions were chosen so that the image would have the correct size to be used as input by the CNN model. The network architecture was U-Net, which performs well in tumor segmentation [77], based on the work developed with automatic lesion segmentation in breast cancer applications specialized in breast US images [78], [79]. The incoming US image is converted, using the OpenCV library, from a 3-channel RGB image to a single-channel grayscale image before being passed to the network, which expects a 512 by 512-pixel wide grayscale image. The network's output is a grayscale image the same size as the input that highlights what it considers to be lesions. Following that, a binary mask is created: using a sigmoid function, the pixels' values are normalized between 0 and 1. Then, pixels with values above a threshold of 0.9 are converted into white pixels, and pixels with values below it are converted into black pixels. This results in a segmentation mask where the segmented lesion is white within a black background. The generated binary mask could detect the lesions most of the time. However, it also identifies image noise as lesions. Fixing this issue was accomplished by calculating a bounding box encompassing every single lesion; the bounding boxes were then ordered by size, and the largest one was assumed to be the lesion. After that, the lesion's position is calculated using its bounding box (Figure 13). The dimensions of the US image may vary in accordance with the US's depth, but the streamed image dimensions remain the same, being filled with transparent pixels. However, we removed these transparent bands, ultimately decreasing the image's width or height.

Communication Protocol

The companion application sends the processed US image and additional information to the AR application. Therefore, a communication protocol was developed to bridge both applications. The choice regarding the communication protocol revolves around the use of TCP or UDP. Although TCP protocol, stream-oriented, is a robust protocol that provides reliability, flow control, and congestion control, it is somewhat slow in terms of performance. On the other hand, the UDP protocol, datagram-oriented, being simpler than TCP,

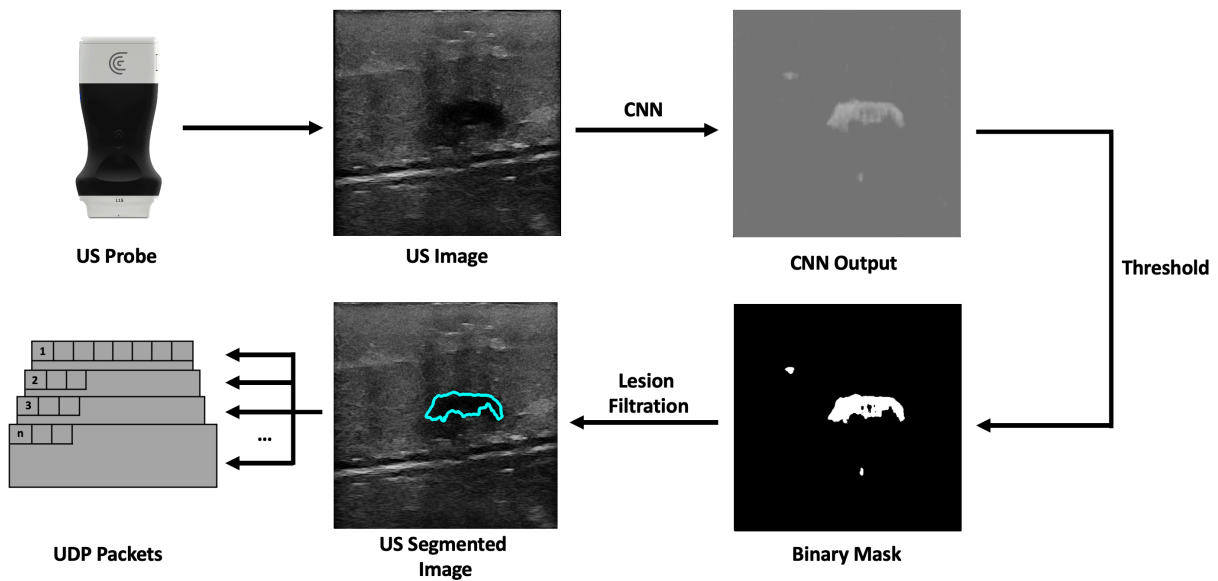


Figure 13: Companion application workflow overview.

since it only guarantees the integrity of packets, and is much more useful for applications where low latency is essential [25], [23]. So, the UDP protocol was chosen as the communication protocol for the task at hand. The datagram protocol devised consists of 512-byte-sized packets that have the US image data partitioned between them. It has i) a header consisting of a 2-byte number that identifies the partition of the image data; ii) an 8-byte US image frame identifier, and iii) 1 byte identifying whether or not that packet is the last one. The receiving application uses the header information to determine when a packet is lost in the communication process. It does this by comparing the current packet number with the last packet number with the same image frame identifier. If the compared numbers are not sequential or the frame identifier is different, the packet sequence is dropped, and the application waits for the next first packet. In addition, the number one packet has additional meta-information about the US image, such as the width and height, the image's pixel spacing, and the predicted lesion center in x and y-pixels.

3.2.3 AR Application

The original idea was, using AR technology to help in the breast biopsy procedure by placing a hologram in the real-world location of the lesion. This would be achieved utilizing the tracking feature to locate the position of the US probe's transducer and the automatic lesion prediction (given by the CNN network) to compute the lesion position to place a hologram there. With this information, the user would try to reach the virtual lesion displayed by the AR glasses. This approach, however, proved to be difficult to use. For starters, the breast might deform with the biopsy needle puncture, and the patient may breathe

or do slight movements with the torso, possibly altering the position of the lesion. In addition, the AR glasses' holograms also provide a misleading sense of depth, which became evident during tests. Hence, a real-time tracking of the biopsy needle was implemented, as well as a real-time display of the real-world position of the lesion. The application was developed to the HoloLens 2 glasses using Unity 3D 2021 [46] (version 2021.3.2f1), Microsoft's Mixed Reality Toolkit for Unity [47], Vuforia AR Software Development Kit (SDK) [49], and Visual Studio 2022.

Needle and US Probe Tracking

Performing the biopsy procedure with the AR glasses aid (Figure 14), requires the localization of its main components, such as the US image, in the 3D world, along with the relative position of the biopsy needle tip. Therefore, the US probe and the biopsy needle require constant tracking by the AR glasses. The solution to actively track both objects revolved around tracking a physical QR code tag mounted on these objects. This is performed utilizing the Vuforia SDK to recognize QR code images in 3D space. The SDK needs prior information of the QR code image and its real-world size. The SDK uses this information to look for pre-determined features on the QR codes. Custom casings were 3D-printed to house the QR code tags on the US probe and on the biopsy needle. These casings were made of polylactic acid and were printed on the Ultimaker II [51] 3D printer with a printing resolution of 0.2mm.

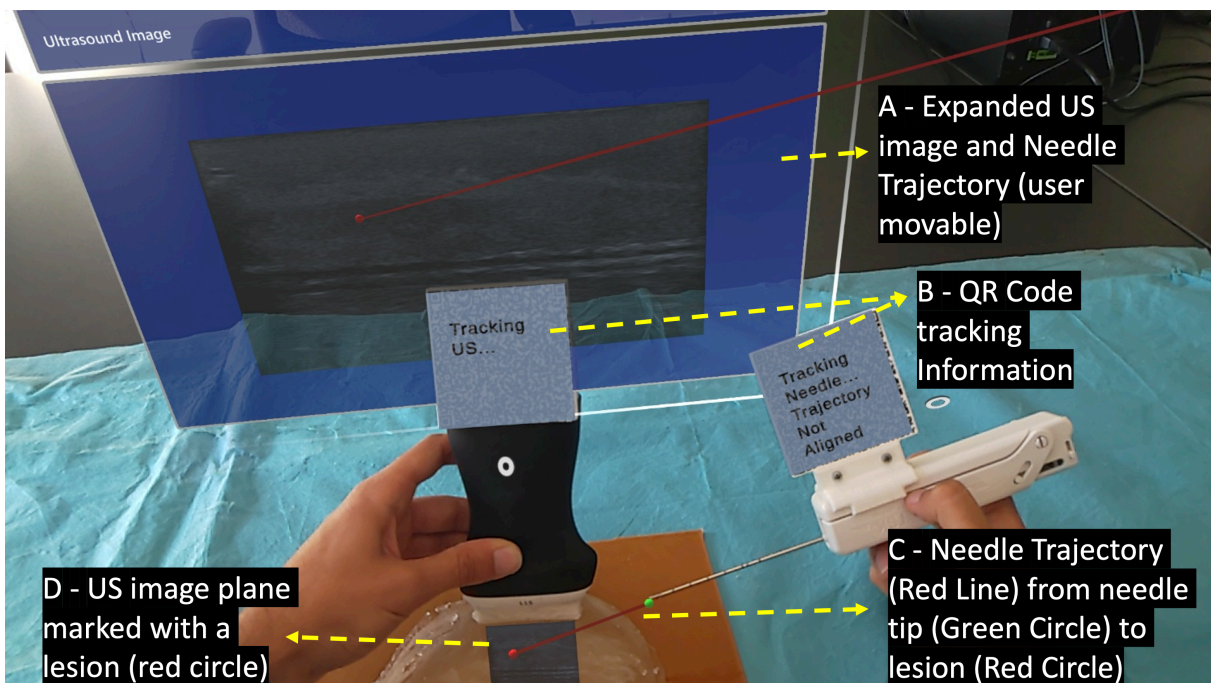


Figure 14: User's point of view performing the biopsy procedure with the AR device.

When the Vuforia SDK is actively tracking a QR code, it places a virtual square hologram, with the

exact dimensions and orientation as the real QR code on top of it to inform the user whether the object is being actively tracked or not. The AR application uses the coordinates of the hologram to access the 3D world position of the QR code. These coordinates represent the center of the QR code tag in the virtual 3D world. By having the QR code tag's center, the real-world size of the 3D printed casing, and the physical object it's mounted on, the application can precisely determine the location of the US probe's transducer and the tip of the biopsy needle.

AR Hologram Generation

The UDP packets received from the companion application contains various segments of an US image that are later combined into a single image hologram. This hologram is resized so its dimensions in the virtual environment match the real-world dimensions. The hologram's dimensions are, therefore, the result of multiplying the image's pixel spacing by its width and height. This hologram is placed right below the US probe's transducer. This hologram may be difficult to visualize on the AR glasses due in part to its small size. Therefore, an expanded version is also displayed to facilitate the visualization. The received lesion center is converted to virtual coordinates by multiplying the x and y components by the image's pixel spacing. A red circle is placed in the lesion center virtual coordinates showing the user where the predicted lesion is.

The physician needs to visualize the needle in real time while performing the US imaging to ensure that the needle will hit the targeted lesion [80]. Therefore, steps have been taken to assist the user in aligning the biopsy needle with the US image plane. This was done by displaying a line from the tracked needle tip to the predicted lesion that changes colors depending on the needle's alignment. The colors vary between green, which indicates alignment, and red, indicating unalignment, as shown in Figure 14C (red line). The calculation of this alignment revolves around the angle between the US image plane and the line that starts at the needle tip and intersects the plane in the predicted lesion location. The ideal angle value is precisely 90° . This value, however, is virtually impossible to reach in the application context due to hand movements and computational uncertainties. An angle range was, therefore, empirically defined, ranging between 86° and 94° .

Using the proposed system, the procedure would start by localizing the lesion in the US image with the help of the CNN segmentation. Then, the user must track the probe and the biopsy needle's QR code tags so the system can calculate the alignment of both elements and guide the biopsy needle to the predicted lesion, using a virtual line than connects them.

3.3 Experiments

3.3.1 Latency and Execution Times

The described prototype relies on real-time calculation to correctly function. Thus, an essential metric to evaluate in the system is latency. In particular, the latency between the US image being generated in the US probe to that image being displayed in the AR system. Therefore, the experiment consisted of marking two distinct positions on a breast phantom and comparing the image's timestamps to compare time differences.

The NDI Polaris Vega ST [81] optical tracker measurements were used as a benchmark to evaluate the latency. The probe was fitted with an optical navigation marker (Figure 15A), and during the experiment, the coordinates of the probe, along with the timestamp of each position, were registered. Meanwhile, AR glasses save the received US images and its timestamps. Since the US images acquired in the two positions are different, it is possible to measure the time difference between the last image of the first position and the first image of the second position (Figure 15). This time difference is compared with the optical tracker data to measure the latency of the AR image displaying system. The latency values were recorded from 10 runs and their average was calculated.

The proposed system has many concurrent operations that collectively account for the overall system's latency. The costliest operations will be evaluated over ten 2-minute runs.

3.3.2 Usability

The developed system prototype could assist either a novice or an experienced physician. Thus, its usability must be simple but effective in aiding the breast biopsy procedure. The assessment of which was made by having 18 people, with a median age of 23.3 years and some or no experience with the biopsy procedure (Figure 16). A custom version of our system was developed, mimicking a traditional biopsy procedure, without any visualization enhancement. However, even in this version, the system needs to track both QR codes to measure the user's accuracy in targeting what the user thinks is a lesion versus the CNN-predicted lesion.

The user is informed of how the biopsy procedure is done and instructed to perform the procedure until they think they have reached the lesion. After using this limited version, the user utilizes the developed prototype. Metrics such as the procedure time, relative angle, and lesion and needle tip location are captured and compared.

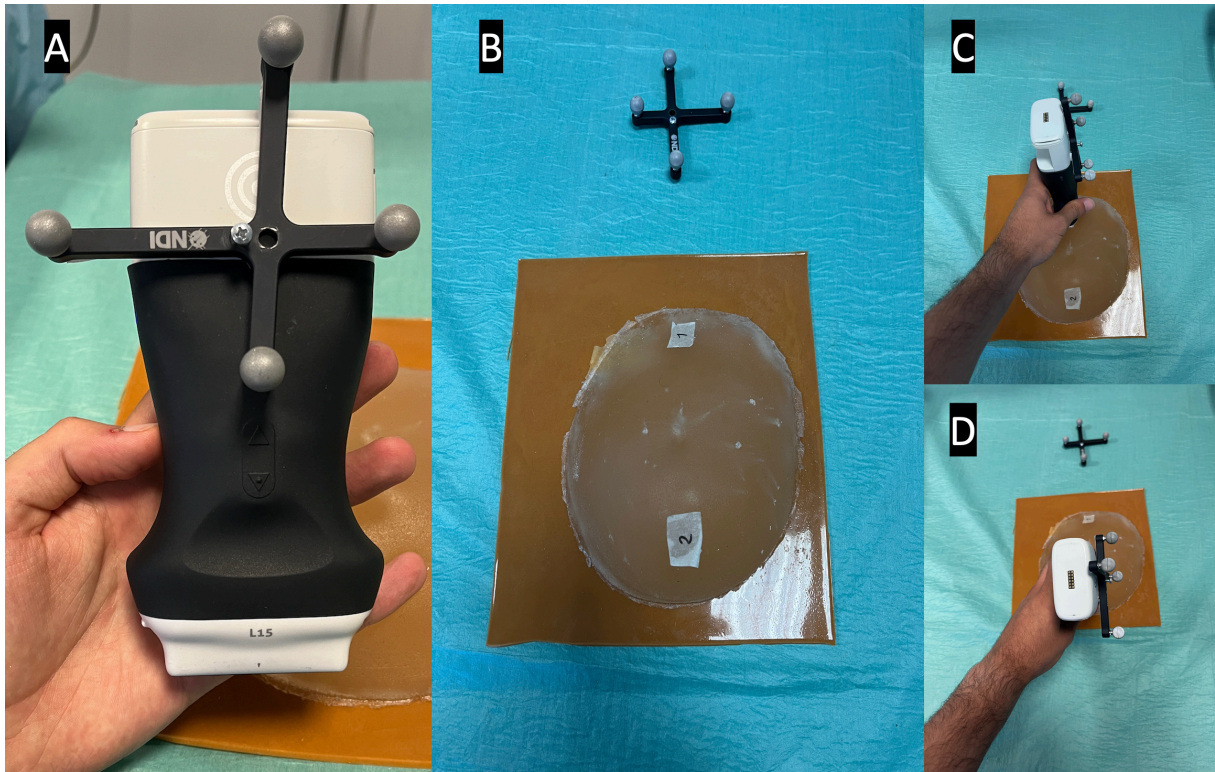


Figure 15: Latency test setup, showing in picture A the optical marker mounted on the US probe, in picture B the breast phantom with both positions marked, and in pictures C and D the US probe in its different test positions.



Figure 16: Third-person usability test view of a user performing the biopsy in a breast phantom.

3.4 Results

3.4.1 Latency and Execution Times

The average time between moving the US probe and that movement being registered in the AR glasses was 143 ± 51.492 milliseconds (ms). Figure 17 shows the latency time data along with the execution times of the observed costliest operations.

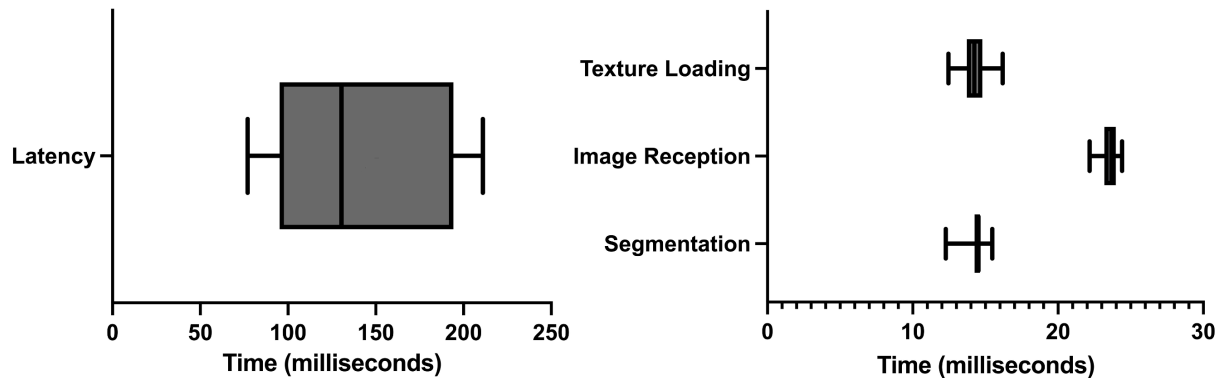


Figure 17: Latency and Execution times.

Of all the different operations, three were observed to be costliest performance-wise: i) the CNN segmentation of the US image; ii) the render time of the US image on the AR glasses, and iii) the time and failure rate in the reception of US images in the AR application. The longest execution time was of the reception of US images in the AR application. On average, it took 23.681 ± 0.637 ms, followed by the US image rendering on the AR application with 14.247 ± 0.953 ms. Finally, the segmentation computing took 14.341 ± 0.831 ms. It was also noted that, on average, 57.3% of the images sent were lost in the communication process.

3.4.2 Usability

The usability test results presented in Figure 18 show that the user, on average, claimed to have completed the biopsy procedure faster in the no-help traditional version, with a time of 33.5 seconds. Our proposed system with needle guidance and lesion prediction took an average of 74.1 seconds. However, the results demonstrate that the user reached the targeted lesion more regularly, with a much lower standard deviation. According to the results acquired, the procedure allowed the users to reach the predicted lesion location more accurately and precisely in our proposed system.

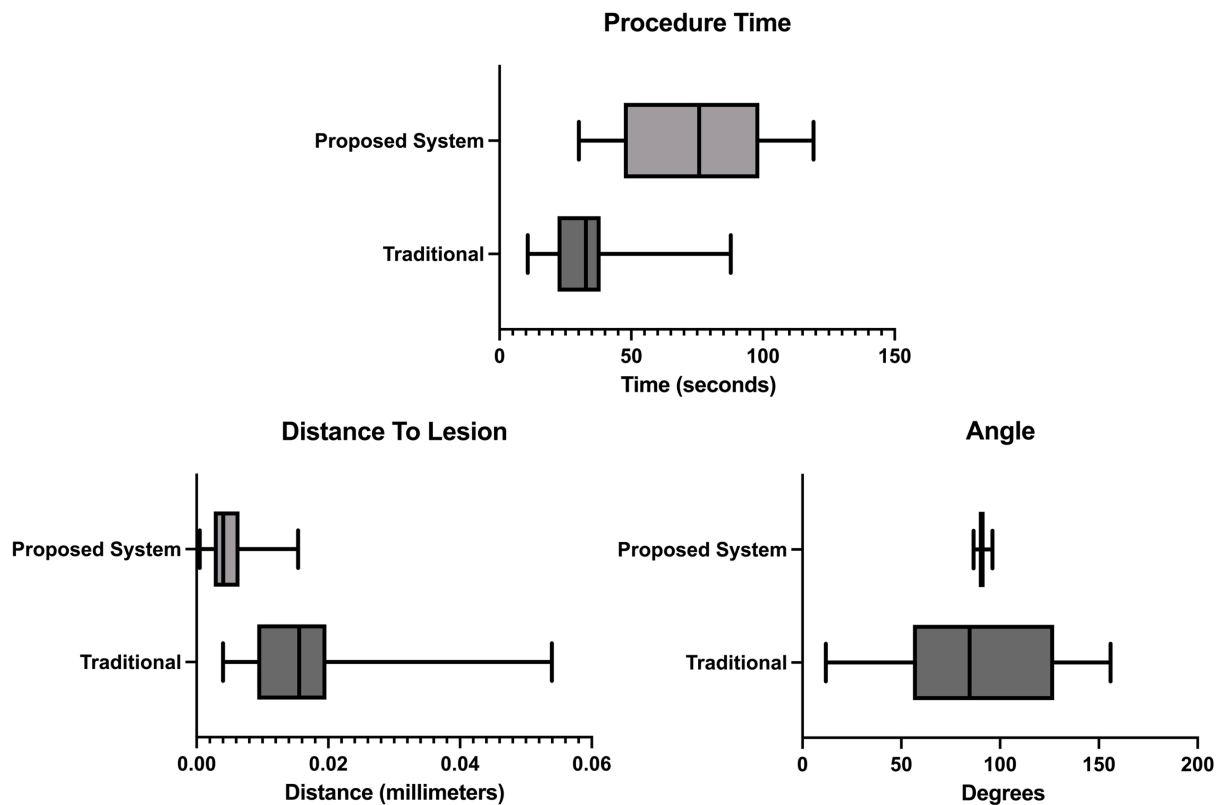


Figure 18: Procedure time, distance from the needle tip to the lesion and angle measurements.

3.5 Discussion

According to the literature, similar solutions have been attempted. The most similar system was developed in 2002 by Rosenthal *et al.* [64]. This solution used dated equipment compared with today's standards and didn't have real-time lesion location prediction. It did, however, prove the concept of using AR as a valuable help in the procedure by having positive physician feedback. Other research have also attempted to use AR glasses as a visualization tool for US images, such as Kashiwagi *et al.* [67] or Nguyen *et al.* [41]. These approaches facilitated hand-eye coordination since users don't need to look away from the US probe's movements to see the US video stream. To the best of our knowledge, no study has presented a technique that uses AR glasses to display real-time video from an US probe while simultaneously displaying lesion prediction from a CNN network and showing the trajectory of the biopsy needle trajectory in real-time.

The results show that the developed prototype has a significant latency of 143ms on average. This value is partly due to the data streaming from the companion application to the AR application via a wireless connection. According to the execution times tests, the computation that lasted longer was the reception of US frames, lasting approximately 23.681ms. However, the failure rate in the reception of US image frames is 57.3%, meaning most frames sent via the network are lost. The approximate US

frame reception time is significantly smaller than the latency value. This phenomenon can be attributed to the extra computation needed for rendering (14.247ms) and CNN image segmentation (14.341ms). The latency time measurements are done by analyzing the received US image frames on the AR application and the timestamp in which they are received, comparing these with the data generated by the optical tracker. However, due to the high failure rate with the communication process, the exact image frame generated in the US probe's second position might be lost, artificially increasing the latency times.

The usability assessment tests showed that the developed prototype improves the overall procedure as opposed to a traditional scenario. For starters, as shown in Figure 18 - Procedure time results, the measured time increases, meaning the users spend more time aligning the biopsy needle with the US image plane. The observed times are higher than the ones obtained in Bluvol *et al.* [82], this may be due to the adaptation to the visualization in the AR glasses. The needle's alignment with the US image became more precise, as noted by the much lower standard deviation value shown in the angle results in Figure 18. These results can be attributed to the implemented angle guidance, which helps the user insert the needle at the optimal angle. The distance between the tip of the needle to the estimated lesion position (distance to lesion results in Figure 18) decreased from 16.25mm in the traditional version to 5.09mm in the proposed version, so it's possible to assume that the process became more precise in the proposed version. The variation in the image segmentation can partially explain this difference. The distance is calculated from the needle tip to a single point that roughly indicates the center of the lesion. However, this point may vary due to slight variations in the US probe's position. The custom no-help application is not the optimal comparison to the developed prototype, as the user needs to wear the AR glasses to track the position of the US probe and the biopsy needle (for comparison with the helped version). The user, however, needed to see the US images on an external display through the AR glasses screen. Possibly hampering the procedure by limiting the visibility of the US video. The system was also tested by a radiologist who gave positive feedback and pointed out that, in the future, it may be used as well as a training device.

3.6 Conclusion

This paper describes and evaluates a solution to aid or be used as a training device for the US-guided breast biopsy procedure. The AR glasses receive US images from a companion application along with lesion segmentation data on each image, which is then displayed in the user's field of view. The application calculates the positions of the US probe's transducer and the biopsy needle tip using the tracking data and

the actual measurements of the objects. This data is combined into a single solution that displays needle tracking and lesion segmentation on the user's field of view. The results show that the proposed solution improves the overall accuracy and precision of the procedure when compared to a traditional system.

As for future work, a new tracking solution must be pursued to cut the reliance on QR codes, which somewhat limit usability during the biopsy procedure. An effort to use an optical tracker is contemplated. With the help of an optical tracker, it would be possible to know the location and orientation of objects, even when hidden from the user's line of sight. The high latency measured and the high failure rate in the image streaming process must also be addressed by improving the communication protocol or experimenting with a wired connection. Additionally, clinical validation will be pursued.

Chapter 4

Proof-of-concept ultrasound biopsy application

4.1 Introduction

This chapter consists of the description of a proof-of-concept software application that was developed within the context of the OncoNavigator framework. Its main objective is to improve the precision of the US-guided breast biopsy procedure. The application (Figure 19) does this by improving the visualization and interpretation of US imaging and controlling a collaborative medical robot to assist with the breast biopsy procedure.

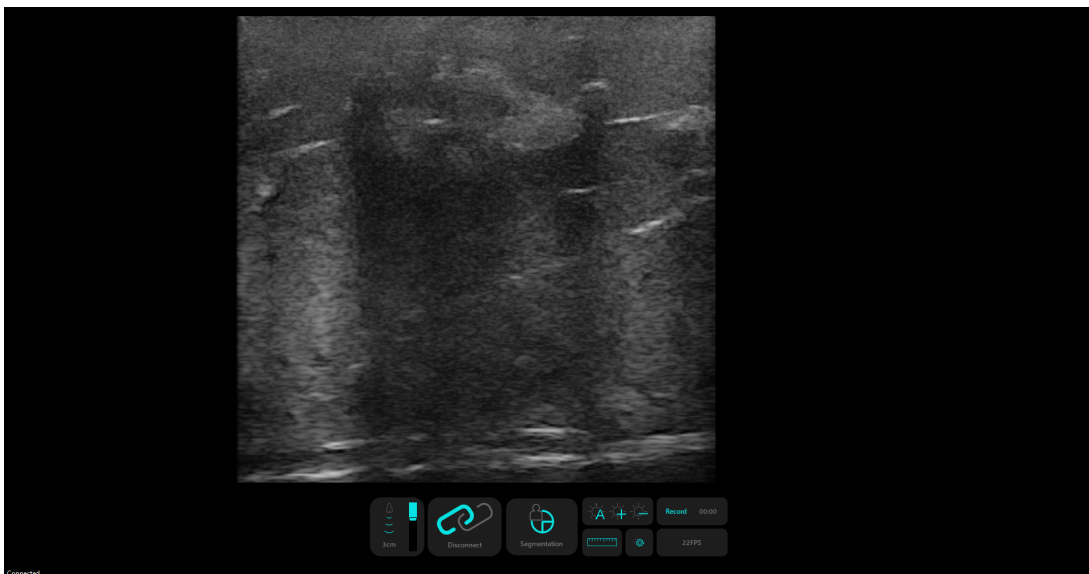


Figure 19: Screenshot of the application's GUI.

The software application's GUI was developed using the Qt 5.15 framework, and US image processing and lesion segmentation were performed using OpenCV 4.5.5 library. The VTK library, version 8.2.0, was also used to display the US images on the screen and to calculate the distance on the US image.

4.2 Developed Features

4.2.1 Ultrasound Specific

The elected US probe was the Clarius L15 HD Portable Handheld Scanner. This probe provides an API for a computing device connection to the real-time US video stream. The usage of this API requires the probe to be connected to the Clarius phone application while at the same time the computing device needs to be connected to the US probe's wi-fi network. The API also allows some of the probe's physical functionalities to be altered, such as the depth and gain parameters.

Ultrasound Imaging Display

The API requires the US probe's IP and port to receive images. These parameters can be changed while the probe is running, as shown in figure 20. By default, the application uses the probe's default values.

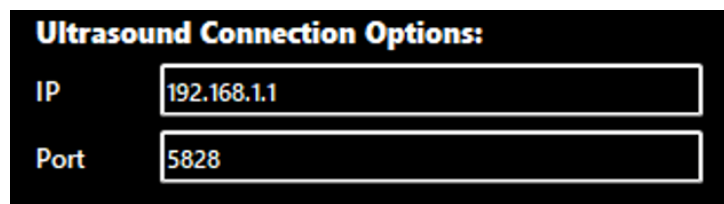


Figure 20: GUI US connection settings .

The connection with the US probe can be made by pressing the connect/disconnect button, highlighted in Figure 21. When a connection is established the application starts receiving and displaying the live US video feed, a screenshot of the application displaying US images can be seen in Figure 19.

Figure 22 shows a workflow diagram of how the application connects to the US probe and Figure 23 shows the us image reception workflow.

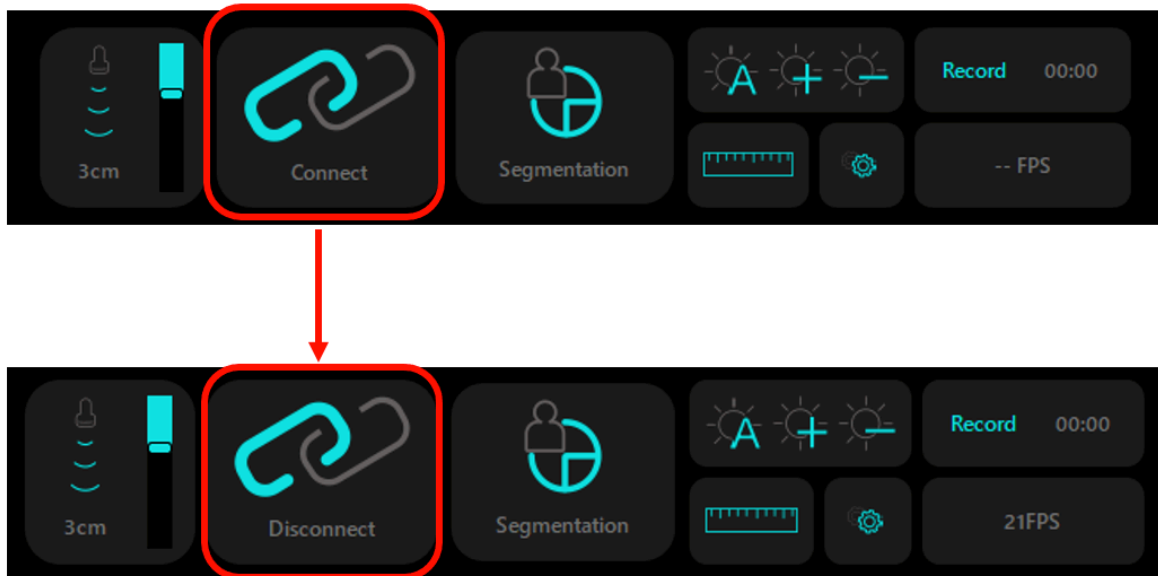


Figure 21: GUI changes when connected to the US probe.

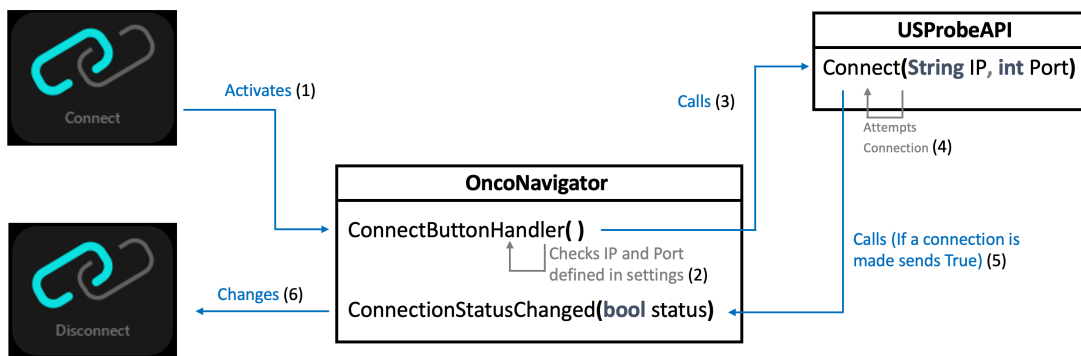


Figure 22: US connection workflow diagram.

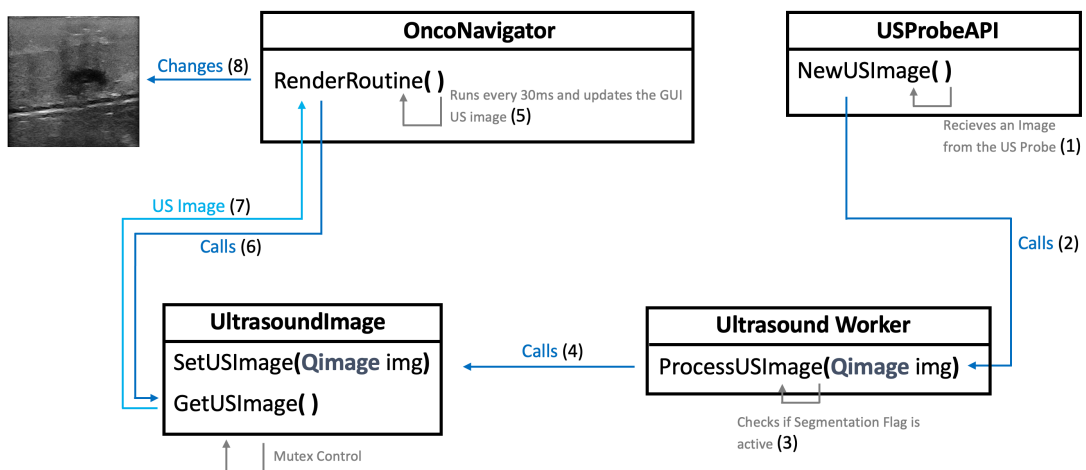


Figure 23: US image reception workflow diagram.

Depth

The utilized US probe allows the user to adjust the US image depth. This value refers to the depth of penetration of the sound rays into the body. It is measured in centimeters, ranging from 1cm to 7cm. Figure 24 shows images acquired with different depths and Figure 25 how the application handles depth change in the form of a workflow diagram.

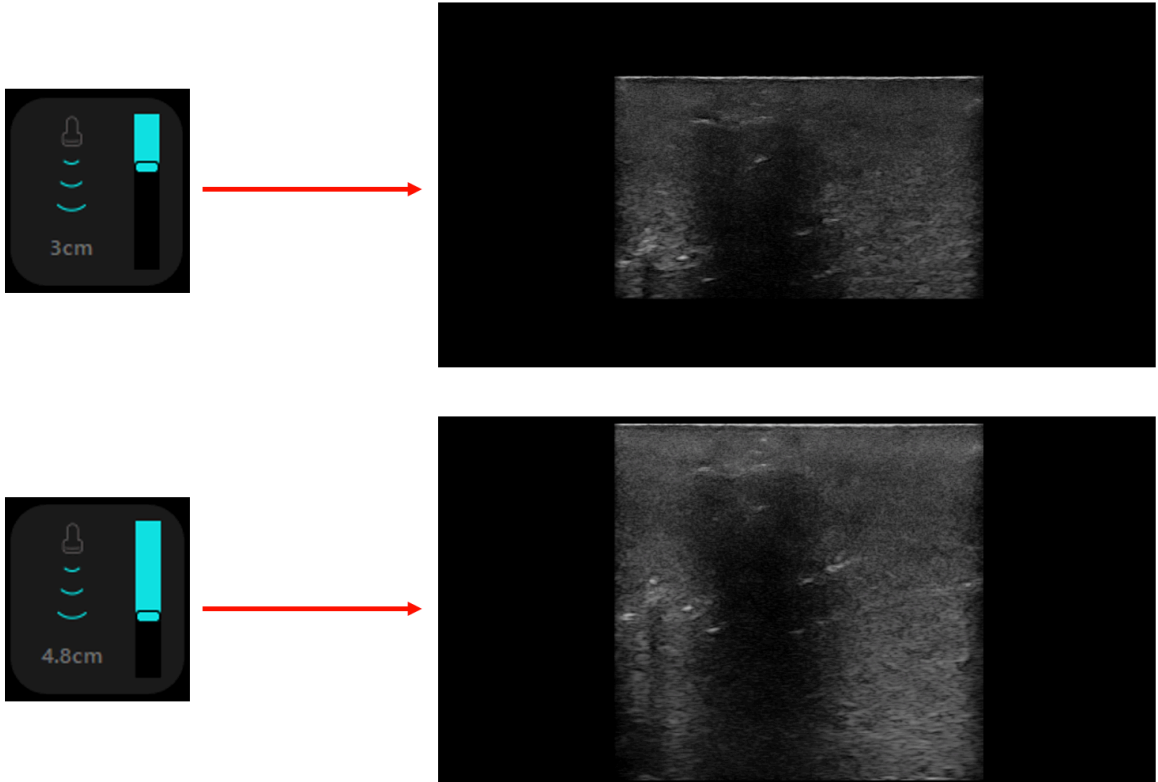


Figure 24: Depth slider user interface and the respective resulting US images.

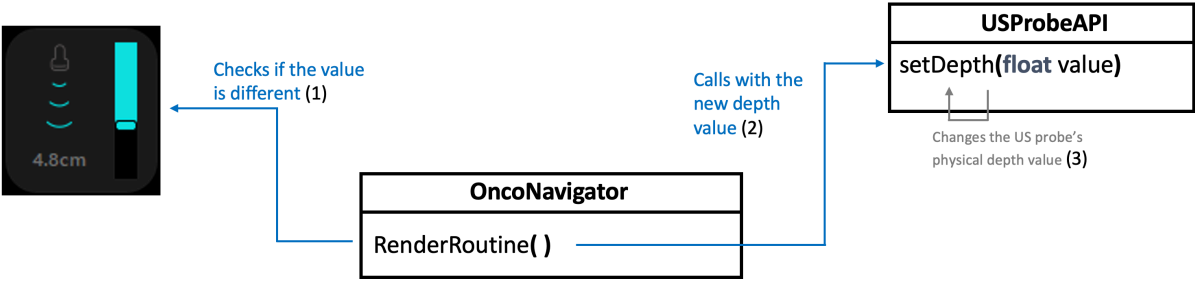


Figure 25: Depth change workflow diagram.

Gain

Gain is a relevant feature and is one of the most used and adjusted scanning parameters. Adjusting the US gain changes the brightness of the image. This change in brightness is due to a uniform amplification of the ultrasonic signal.

The US probe allows increasing, decreasing, and toggling auto-gain in its API. These commands are available as buttons representing these features, as shown in figure 26. Figure 27 shows in a diagram how the gain buttons work in the context of the application.

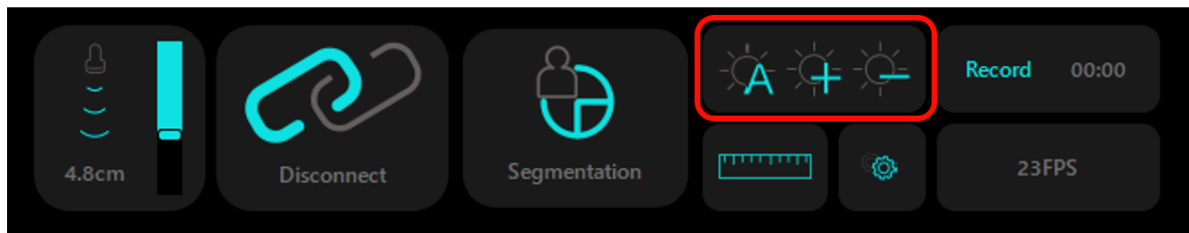


Figure 26: Gain setting buttons.

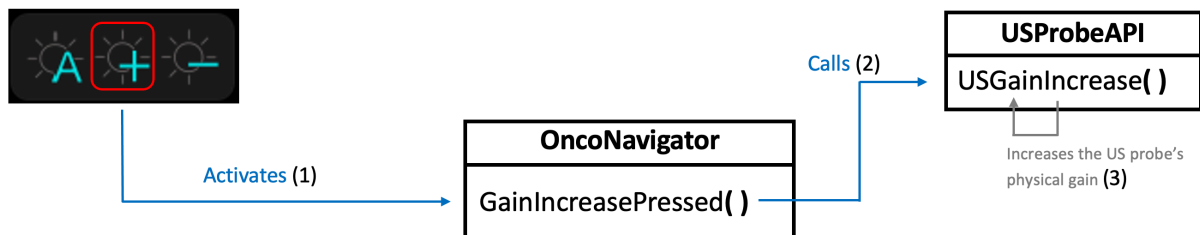


Figure 27: Gain change workflow diagram.

4.2.2 Collaborative Robot Control

The OncoNavigator project aims to use a collaborative medical robot to hold an US probe to a custom-made gripper. The robot is used to fix the US probe in a user-defined position that accounts for user breathing movements.

The software application uses the 3D connexion's Space Mouse Compact to control the robot's movements. The application connects to the mouse and accesses its data by sending it 4 bytes and receiving 28 bytes back. The data that it receives has an indication if any of the mouse's buttons were pressed and six values with the translational and rotational data of the mouse's joystick. The robot system is also connected to the application and gets its data by sending 4 bytes to the application and receiving 26 bytes back, with the latest obtained translational and rotational data of the mouse.

An illustration of the exchange of data between the mouse, application and the robot is displayed in Figure 28.

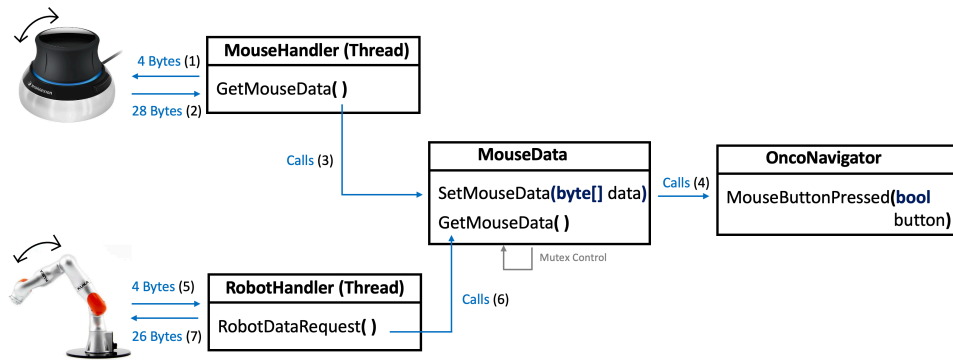


Figure 28: Robot control workflow diagram.

4.2.3 Usability

Segmentation

The segmentation feature is explained in detail in the developed companion application section 3.2.2 and in figure 13. In short, it uses the US probe's API to receive a live US video feed. These images are then passed through a convolutional neural network, and the resulting output is overlaid over the US image, highlighting the predicted lesions. The segmentation button and the segmentation (in green) overlaying the lesion are shown in Figure 29. Figure 30 shows how the segmentation is handled in the application.

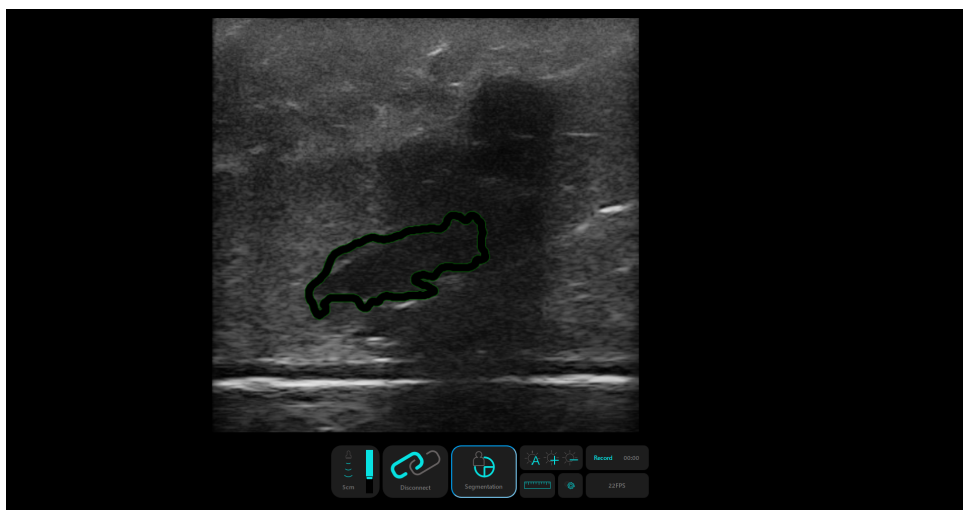


Figure 29: Segmentation overlay feature.

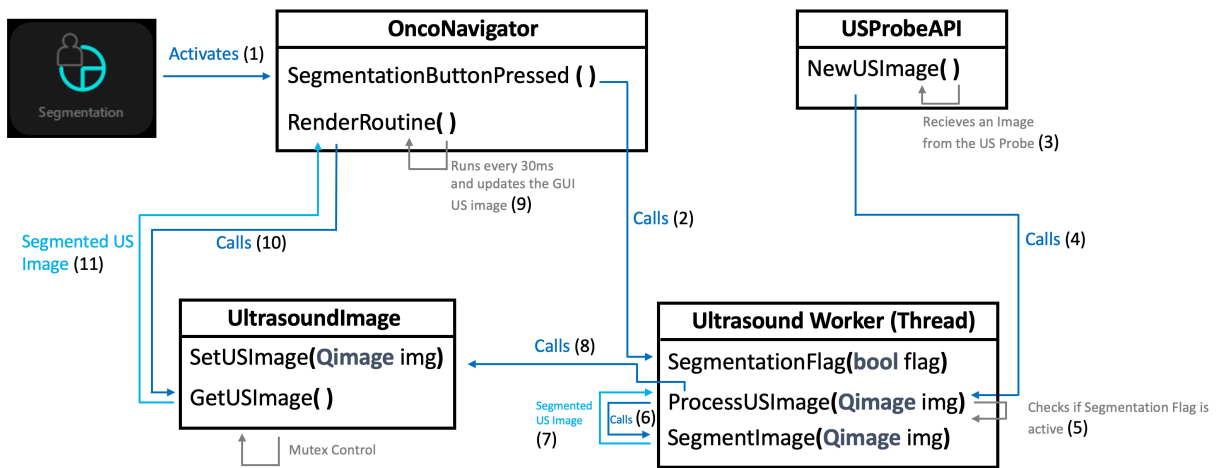


Figure 30: Segmentation activation workflow diagram.

Video Recording and Image Capture

The implementation of US image capture was carried out. This capture either as a video or as a screenshot. Ultrasound exams can be easily stored and later added to a patient's clinical history.

The recorded information is stored in a predetermined folder on the computing device, but this saving location can be changed later in the settings. Video capture settings such as FPS or resolution can also be altered, as shown in figure 31.

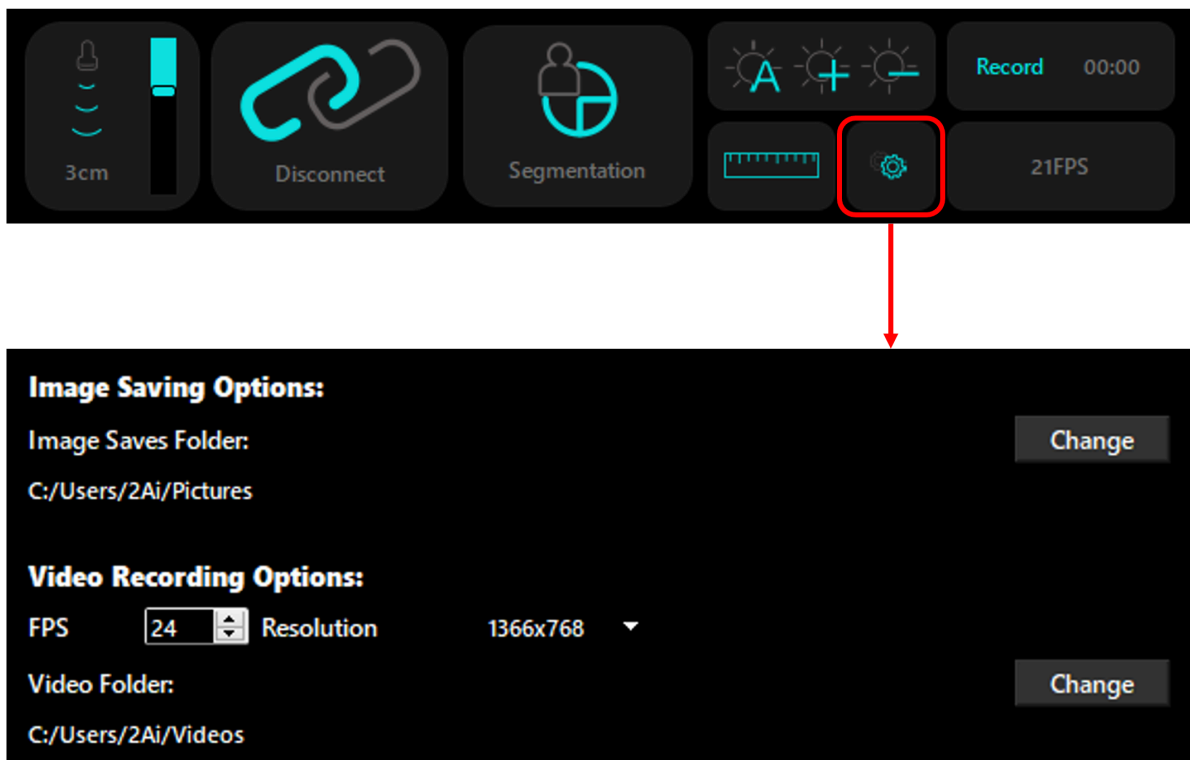


Figure 31: Video recording and image screenshot setting options.

Ultrasound video can be recorded by pressing the Record button on the bottom menu. The video length starts counting upwards, so the user can know the duration of the video. The video is recorded at the settings-defined FPS and up-scales the US image to fit the pre-determined resolution. To stop the recording the user presses the stop button and the video is saved into a file in the designated folder. This process is shown in Figure 32. The inner workings of the recording process in the application can be shown in Figures 33 and 34.

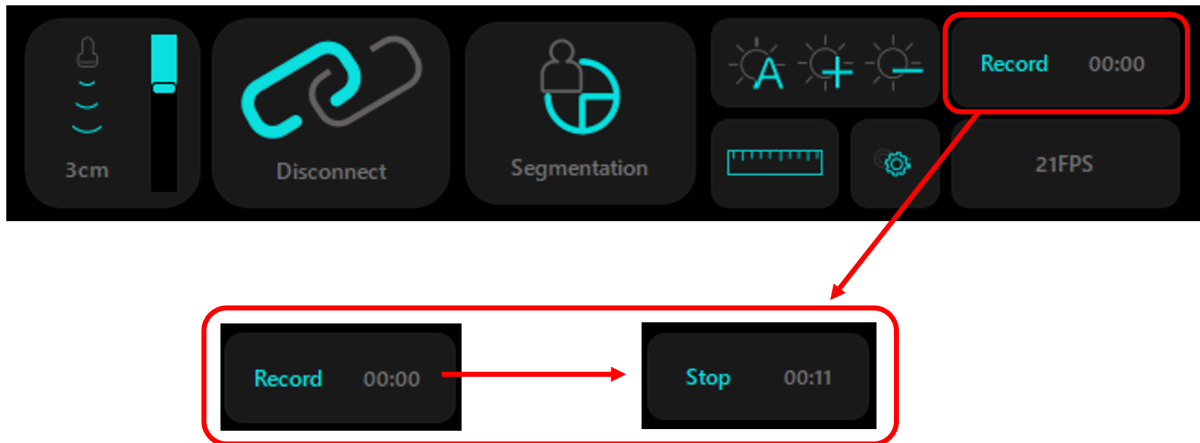


Figure 32: Video recording in practice.

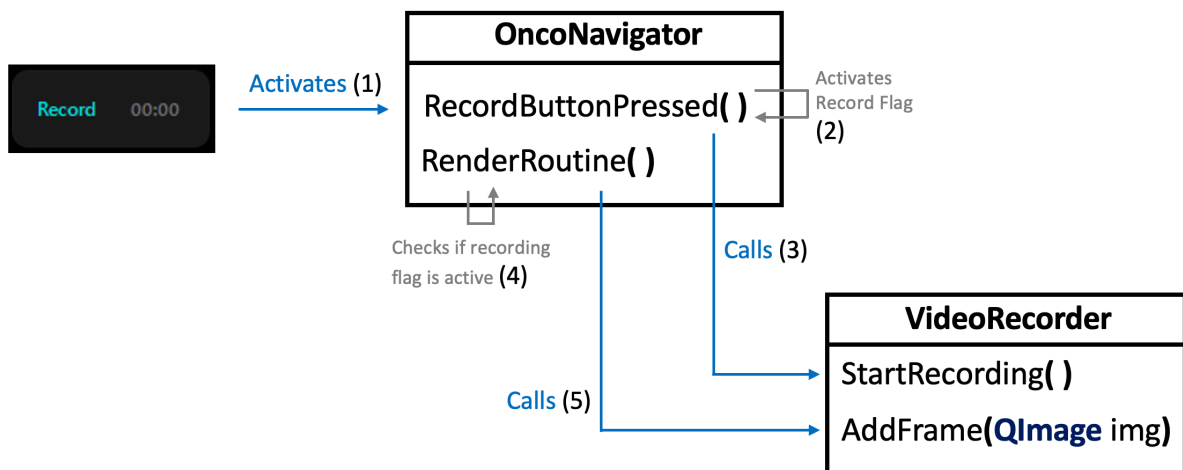


Figure 33: Recording process start workflow diagram.

Images can be saved by pressing a physical button on the US probe. This raises a flag on the software and signals that the next incoming US image needs to be stored on the disk. Figure 35 shows a diagram representation of how a screenshot is saved from pressing the physical probe's button to the US image being saved onto the disk.

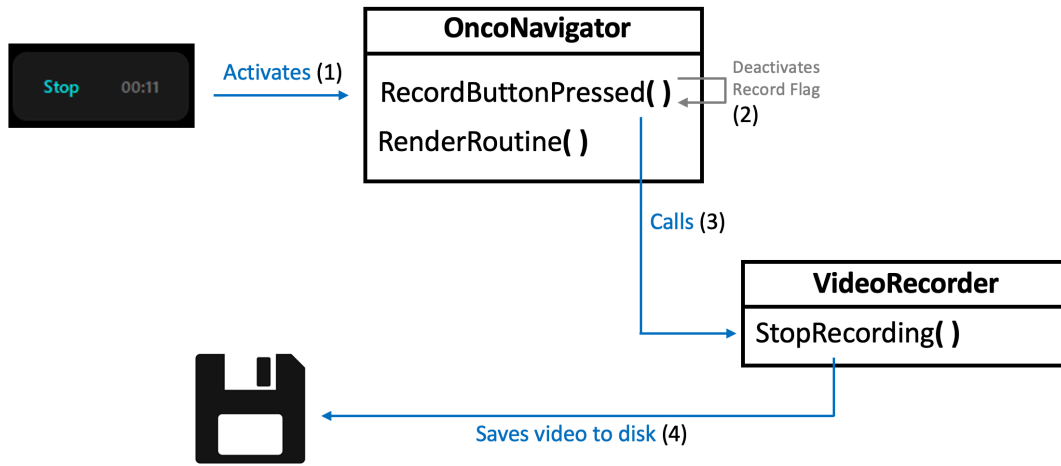


Figure 34: End recording workflow diagram.

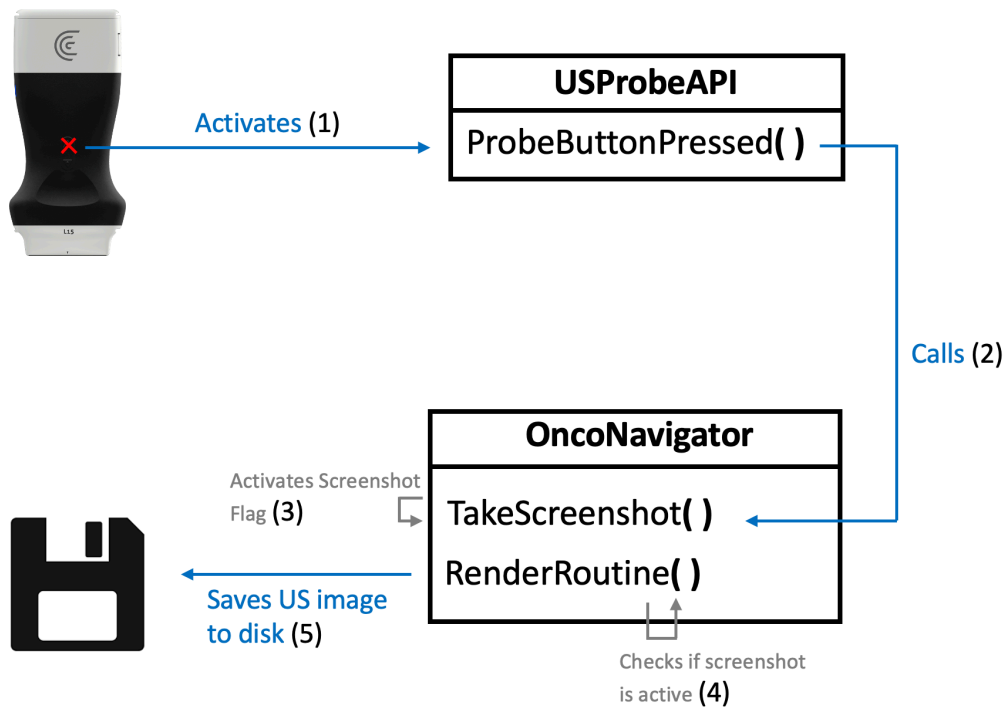


Figure 35: Screenshot workflow diagram.

Distance Widget

The software has been enhanced with a measuring tool. It uses the US image's pixel spacing to take accurate real-world measurements. The implementation of which was done with a VTK distance widget, that controls the mouse clicks. The provided image's pixel spacing is applied to the virtual pixel distance, and the result is displayed in millimeters, as shown in Figure 36. Figure 37 shows the distance widget activation workflow.

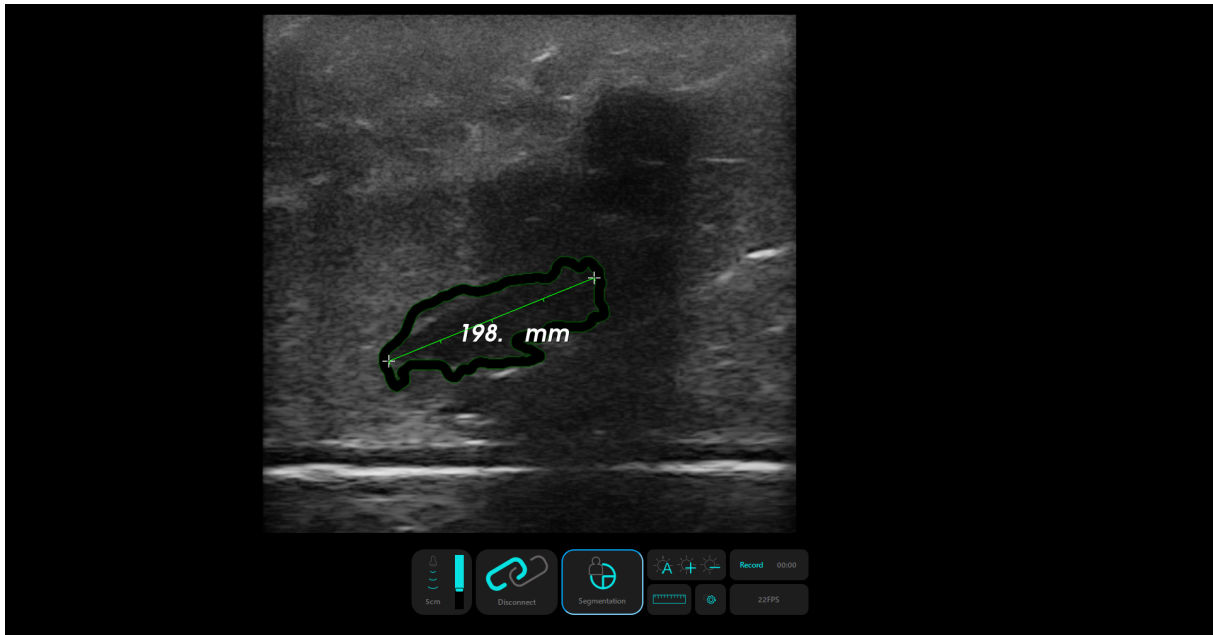


Figure 36: Distance widget display.

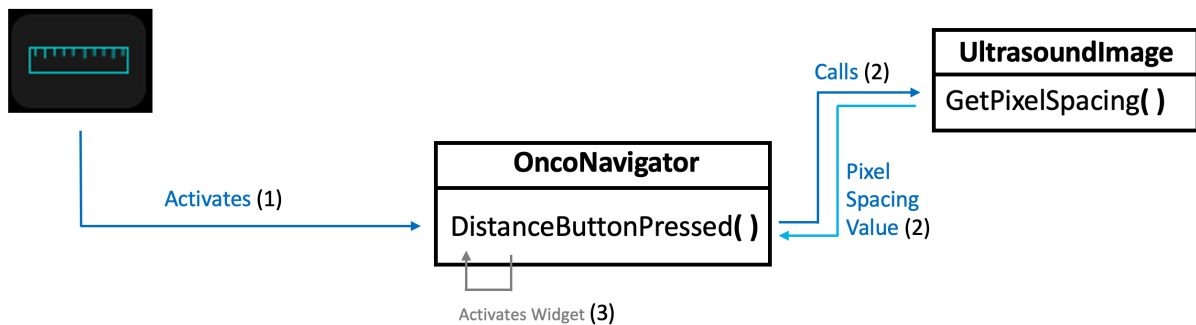


Figure 37: Distance tool activation workflow diagram.

4.3 Discussion

This application is part of the OncoNavigator framework, and one of its purposes is the integration of other developed components, such as the trajectory and segmentation components.

The software runs smoothly and has real-time capabilities. A custom-made FPS counter that computes how many US frames the application can render in a second was integrated. The FPS count was at a constant rate of 23, regardless of whether segmentation was on or off. This shows that the segmentation calculation has no impact on the overall performance of the application.

It should be noted that the physical sensor that would measure the orientation and displacement of the biopsy needle suffered several delays and setbacks. With this in mind, the development of the needle trajectory display had to be removed (for the time being).

As for future work, a needle trajectory display solution will be implemented to enhance the prototype of this application. Then, an attempt will be made to provide access to the physical location of the US probe, lesion, breast, and biopsy needle. This would ensure that it displays a more faithful representation of the procedure to the physician.

Chapter 5

Conclusion

The dissertation describes the work developed within the OncoNavigator navigation system. This work is focused on improving the US-guided breast biopsy, either by enhancing medical training with novel displaying techniques or improving the precision of physicians with the procedure.

Using the HoloLens 2 AR glasses, an US simulator was developed. This simulator features a tracking system for the US probe using the cameras built into the AR glasses. Its orientation is captured and used to compute an US image, which is displayed on the glasses. The glasses' tracking capabilities were compared with an electromagnetic tracking device, and similar results were observed. These results support the use of AR glasses as a assistive device to be used in breast biopsy. A research paper describing this work was published at an international conference, and its contents are present in this dissertation.

The experience acquired with the AR US simulator led to the development of a breast biopsy system using AR as a visualization tool. The prototype displays the needle trajectory along with real-time lesion segmentation. A research paper, soon to be published, describes this work. Its contents are also present in this dissertation. An experiment that consisted of users being asked to complete the biopsy procedure was carried out. This experiment was done with a preliminary version of the software, with no guidance or help, and later with the developed prototype. Data was captured in both attempts and the results were positive. On average, the procedure became more accurate and precise with the developed prototype.

With the breast biopsy procedure in mind, a software application was developed. It displays real-time US imaging along with segmentation to help as a visualization tool for the physician. The application presented good performance and is an alternative to the aforementioned AR solution.

The main objectives outlined in this dissertation were accomplished and published. The breast biopsy procedure was aided by automatic lesion segmentation and enhancement of the needle trajectory. When compared to the traditional procedure, the AR solution developed proved to be more accurate and precise, and useful as a medical training tool.

As for future work, research must be pursued on different tracking solutions, so objects can still be

tracked even when they're out of the user's sight. Latency and execution times must likewise be improved, by experimenting with different communication protocols or using more efficient code on the AR glasses. Finally, further validation and endurance testing will be pursued, along with the implementation of a needle trajectory display solution on the OncoNavigator proof-of-concept application.

References

- [1] Yuliana Jiménez-gaona, María José Rodríguez-álvarez, and Vasudevan Lakshminarayanan. Deep-learning-based computer-aided systems for breast cancer imaging: A critical review. *Applied Sciences (Switzerland)*, 10(22):1–29, 2020.
- [2] Young Eun Kim, Joo Hee Cha, Hak Hee Kim, Hee Jung Shin, Eun Young Chae, and Woo Jung Choi. The accuracy of mammography, ultrasound, and magnetic resonance imaging for the measurement of invasive breast cancer with extensive intraductal components. *Clinical Breast Cancer*, 10 2022.
- [3] Nicole S Winkler. Ultrasound guided core breast biopsies. *Techniques in Vascular and Interventional Radiology*, 24:100776, 9 2021.
- [4] Zohre Momenimovahed and Hamid Salehiniya. Epidemiological characteristics of and risk factors for breast cancer in the world. *Breast Cancer: Targets and Therapy*, Volume 11:151–164, 4 2019.
- [5] John E. Skandalakis. Embryology and Anatomy of the Breast. In *Breast Augmentation*, pages 3–24. Springer Berlin Heidelberg, Berlin, Heidelberg, 2009.
- [6] Sergiusz Łukasiewicz, Marcin Czeczelewski, Alicja Forma, Jacek Baj, Robert Sitarz, and Andrzej Stanisławek. Breast cancer—epidemiology, risk factors, classification, prognostic markers, and current treatment strategies—an updated review. *Cancers*, 13:4287, 8 2021.
- [7] Shaoyuan Lei, Rongshou Zheng, Siwei Zhang, Shaoming Wang, Ru Chen, Kexin Sun, Hongmei Zeng, Jiachen Zhou, and Wenqiang Wei. Global patterns of breast cancer incidence and mortality: A population-based cancer registry data analysis from 2000 to 2020. *Cancer Communications*, 41:1183–1194, 11 2021.
- [8] Scott Mayer McKinney, Marcin Sieniek, Varun Godbole, Jonathan Godwin, Natasha Antropova, Hutan Ashrafian, Trevor Back, Mary Chesus, Greg C. Corrado, Ara Darzi, Mozziyar Etemadi, Florencia Garcia-Vicente, Fiona J. Gilbert, Mark Halling-Brown, Demis Hassabis, Sunny Jansen, Alan Karthikesalingam, Christopher J. Kelly, Dominic King, Joseph R. Ledsam, David Melnick, Hormuz Mostofi,

- Lily Peng, Joshua Jay Reicher, Bernardino Romera-Paredes, Richard Sidebottom, Mustafa Suleyman, Daniel Tse, Kenneth C. Young, Jeffrey De Fauw, and Shravya Shetty. International evaluation of an AI system for breast cancer screening. *Nature* 2020 577:7788, 577(7788):89–94, jan 2020.
- [9] Zohre Momenimovahed and Hamid Salehiniya. Epidemiological characteristics of and risk factors for breast cancer in the world. *Breast Cancer: Targets and Therapy*, 11:151–164, apr 2019.
- [10] Lulu Wang. Early diagnosis of breast cancer. *Sensors (Switzerland)*, 17(7), 2017.
- [11] Kenneth R. Tomkovich. Interventional radiology in the diagnosis and treatment of diseases of the breast: A historical review and future perspective based on currently available techniques. *American Journal of Roentgenology*, 203:725–733, 10 2014.
- [12] Ulrich Bick et al. Image-guided breast biopsy and localisation: recommendations for information to women and referring physicians by the European Society of Breast Imaging. *Insights into Imaging*, 11(1), 2020.
- [13] Mustafa Z. Mahmoud, Mohammed Aslam, Mohammed Alsaadi, Maram A. Fagiri, and Batil Alonazi. Evolution of Robot-assisted ultrasound-guided breast biopsy systems. *Journal of Radiation Research and Applied Sciences*, 11(1):89–97, jan 2018.
- [14] Tamas Ungi, Andras Lasso, and Gabor Fichtinger. Open-source platforms for navigated image-guided interventions. *Medical Image Analysis*, 33:181–186, oct 2016.
- [15] Ivo Wolf, Marcus Vetter, Ingmar Wegner, Marco Nolden, Thomas Bottger, Mark Hastenteufel, Max Schobinger, Tobias Kunert, and Hans-Peter Meinzer. The medical imaging interaction toolkit (MITK): a toolkit facilitating the creation of interactive software by extending VTK and ITK. *Medical Imaging 2004: Visualization, Image-Guided Procedures, and Display*, 5367:16–27, may 2004.
- [16] A. M. Franz, A. Seitel, M. Servatius, C. Zöllner, I. Gergel, I. Wegner, J. Neuhaus, S. Zelzer, M. Nolden, J. Gaa, P. Mercea, K. Yung, C. M. Sommer, B. A. Radeleff, H.-P. Schlemmer, H.-U. Kauczor, H.-P. Meinzer, and L. Maier-Hein. Simplified development of image-guided therapy software with MITK-IGT. *Medical Imaging 2012: Image-Guided Procedures, Robotic Interventions, and Modeling*, 8316:762–769, feb 2012.
- [17] Marco Nolden, Sascha Zelzer, Alexander Seitel, Diana Wald, Michael Müller, Alfred M. Franz, Daniel Maleike, Markus Fangerau, Matthias Baumhauer, Lena Maier-Hein, Klaus H. Maier-Hein, Hans Peter

- Meinzer, and Ivo Wolf. The medical imaging interaction toolkit: Challenges and advances: 10 years of open-source development. *International Journal of Computer Assisted Radiology and Surgery*, 8(4):607–620, apr 2013.
- [18] Andriy Fedorov, Reinhard Beichel, Jayashree Kalpathy-Cramer, Julien Finet, Jean Christophe Fillion-Robin, Sonia Pujol, Christian Bauer, Dominique Jennings, Fiona Fennessy, Milan Sonka, John Buatti, Stephen Aylward, James V. Miller, Steve Pieper, and Ron Kikinis. 3D Slicer as an image computing platform for the Quantitative Imaging Network. *Magnetic Resonance Imaging*, 30(9):1323–1341, nov 2012.
- [19] Christian Askeland, Ole Vegard Solberg, Janne Beate Lervik Bakeng, Ingerid Reinertsen, Geir Arne Tangen, Erlend Fagertun Hofstad, Daniel Høyer Iversen, Cecilie Våpenstad, Tormod Selbekk, Thomas Langø, Toril A. Nagelhus Hernes, Håkon Olav Leira, Geirmund Unsgård, and Frank Lindseth. CustusX: an open-source research platform for image-guided therapy. *International Journal of Computer Assisted Radiology and Surgery*, 11(4):505–519, apr 2016.
- [20] Shadie R. Badaan and Dan Stoianovici. *Robotic Systems: Past, Present, and Future*, pages 655–665. Springer London, London, 2011.
- [21] Giuseppe Megali, Oliver Tonet, Cesare Stefanini, Mauro Boccadoro, Vassilios Papaspyropoulos, Licinio Angelini, and Paolo Dario. A computer-assisted robotic ultrasound-guided biopsy system for video-assisted surgery. *Lecture Notes in Computer Science (including subseries Lecture Notes in Artificial Intelligence and Lecture Notes in Bioinformatics)*, 2208:343–350, 2001.
- [22] Momen Abayazid, Pedro Moreira, Navid Shahriari, Sachin Patil, Ron Alterovitz, and Sarthak Misra. Ultrasound-guided three-dimensional needle steering in biological tissue with curved surfaces. *Medical Engineering and Physics*, 37:145–150, 1 2015.
- [23] James F. Kurose and Keith W. Ross. *Computer networking: a top-down approach*. Addison-Wesley, 2010.
- [24] Albandari Mishal Alotaibi, Bedour Fahaad Alrashidi, Samina Naz, and Zahida Parveen. Security issues in Protocols of TCP/IP Model at Layers Level. *International Journal of Computer Networks and Communications Security*, 5(5):96–104, 2017.
- [25] W. Richard Stevens and Gary R. Wright. *TCP/IP Illustrated (3 Volume Set)*. Addison-Wesley Professional, 2001.

- [26] Santosh Kumar and Sonam Rai. Survey on Transport Layer Protocols: TCP & UDP. *International Journal of Computer Applications*, 46(7):975–8887, 2012.
- [27] Fahad Taha Al-Dhief, Naseer Sabri, N. M. Abdul Latiff, Nik Noordini Nik Abd Malik, Musatafa Abbas Abbood Albader, Mazin Abed Mohammed, Rami Noori Al-Haddad, Yasir Dawood Salman, Mohd Khanapi Abd Ghani, and Omar Ibrahim Obaid. Performance comparison between TCP and udp protocols in different simulation scenarios. *International Journal of Engineering and Technology(UAE)*, 7(4.36 Special Issue 36):172–176, 2018.
- [28] Junichi Tokuda, Gregory S. Fischer, Xenophon Papademetris, Ziv Yaniv, Luis Ibanez, Patrick Cheng, Haiying Liu, Jack Blevins, Jumpei Arata, Alexandra J. Golby, Tina Kapur, Steve Pieper, Everette C. Burdette, Gabor Fichtinger, Clare M. Tempny, and Nobuhiko Hata. OpenIGTLink: An open network protocol for image-guided therapy environment. *International Journal of Medical Robotics and Computer Assisted Surgery*, 5(4):423–434, 2009.
- [29] Andras Lasso, Tamas Heffter, Adam Rankin, Csaba Pinter, Tamas Ungi, and Gabor Fichtinger. PLUS: Open-source toolkit for ultrasound-guided intervention systems. *IEEE Transactions on Biomedical Engineering*, 61(10):2527–2537, oct 2014.
- [30] Tobias Frank, Axel Krieger, Simon Leonard, Niravkumar A. Patel, and Junichi Tokuda. ROS-IGTL-Bridge: an open network interface for image-guided therapy using the ROS environment. *International Journal of Computer Assisted Radiology and Surgery*, 12(8):1451–1460, aug 2017.
- [31] Alexander Schoch, Bernhard Fuerst, Felix Achilles, Stefanie Demirci, and Nassir Navab. A Lightweight and Portable Communication Framework for Multimodal Image-Guided Therapy. *The MIDAS Journal*, pages 1–8, aug 2013.
- [32] Martin G. Tolsgaard, Tobias Todsén, Jette L. Sørensen, Charlotte Ringsted, Torben Lorentzen, Bent Ottesen, and Ann Tabor. International multispecialty consensus on how to evaluate ultrasound competence: A delphi consensus survey. *PLoS ONE*, 8:e57687, 2 2013.
- [33] Simao Valente, Antonio Real, Joao Gomes-Fonseca, Helena R. Torres, Estevao Lima, Pedro Morais, and Joao L. Vilaca. A new handheld ultrasound probe simulator for medical training. pages 1–7. IEEE, 8 2021.
- [34] "Ultraschall - ultrasound training simulator", <https://medsim.com/ultrasim.html> - Accessed on Jan. 20, 2022.

- [35] "Simulation - Intelligent Ultrasound", <https://www.intelligentultrasound.com/simulation/> - Accessed on Jan. 20, 2022.
- [36] "Ultrasound Education - Easy. Convenient. Effective. - SonoSim Ultrasound Training Solution", <https://sonosim.com/ultrasound-training/> - Accessed on Jan. 20, 2022.
- [37] "CAE Vimedix | CAE Healthcare", <https://www.caehealthcare.com/ultrasound-simulation/vimedix/> - Accessed on Jan. 20, 2022.
- [38] "Ultrasound Simulator | Innoging", <https://ultrasound-simulator.com/> - Accessed on Jan. 20, 2022.
- [39] "diSplay U/S - Online ultrasound simulator by InSimo", <https://www.insimo.com/display-ultrasound/> - Accessed on Jan. 20, 2022.
- [40] Faraz Mahmood, Eitezaz Mahmood, Robert Gregory Dorfman, John Mitchell, Feroze-Udin Mahmood, Stephanie B. Jones, and Robina Matyal. Augmented reality and ultrasound education: Initial experience. *Journal of Cardiothoracic and Vascular Anesthesia*, 32:1363–1367, 6 2018.
- [41] Trong Nguyen, William Plishker, Andrew Matisoff, Karun Sharma, and Raj Shekhar. Holous: Augmented reality visualization of live ultrasound images using hololens for ultrasound-guided procedures. *International Journal of Computer Assisted Radiology and Surgery*, 11 2021.
- [42] Henry Fuchs, Andrei State, Etta D. Pisano, William F. Garrett, Gentaro Hirota, Mark Livingston, Mary C. Whitton, and Stephen M. Pizer. Towards performing ultrasound-guided needle biopsies from within a head-mounted display, 1996.
- [43] Tobias Blum, Sandro Michael Heining, Oliver Kutter, and Nassir Navab. Advanced training methods using an augmented reality ultrasound simulator. pages 177–178. IEEE, 10 2009.
- [44] "Microsoft HoloLens | Mixed Reality Technology for Business", <https://www.microsoft.com/en-us/hololens> - Accessed on Sep. 26, 2022.
- [45] "High-Frequency Linear Scanner | Clarius", <https://clarius.com/scanners/l115/> - Accessed on Sep. 26, 2022.
- [46] "Unity Real-Time Development Platform | 3D, 2D VR & AR Engine", <https://unity.com/> - Accessed on Sep. 26, 2022.

- [47] "MRTK2-Unity Developer Documentation - MRTK 2 | Microsoft Learn", <https://learn.microsoft.com/en-us/windows/mixed-reality/mrtk-unity/mrtk2/> - Accessed on Sep. 26, 2022.
- [48] "Visual Studio: IDE and Code Editor for Software Developers and Teams", <https://visualstudio.microsoft.com/> - Accessed on Oct. 20, 2022.
- [49] "Vuforia Developer Portal", <https://developer.vuforia.com/> - Accessed on Sep. 26, 2022.
- [50] "Image Targets | VuforiaLibrary", <https://library.vuforia.com/features/images/image-targets.html> - Accessed on Aug. 13, 2022.
- [51] "Ultimaker 2+ Connect: Start 3D printing the Ultimaker way", <https://ultimaker.com/3d-printers/ultimaker-2-plus-connect> - Accessed on Sep. 26, 2022.
- [52] "SOLIDWORKS", <https://www.solidworks.com/> - Accessed on Oct. 20, 2022.
- [53] "GN640 | NON-METAL LASER ENGRAVING CUTTING MACHINE / GBOS LASER", <https://www.gboslaser.com/products/gn640-1> - Accessed on Oct. 20, 2022.
- [54] "Aurora - NDI", <https://www.ndigital.com/electromagnetic-tracking-technology/aurora/> - Accessed on Oct. 20, 2022.
- [55] "MATLAB - MathWorks - MATLAB & Simulink", <https://www.mathworks.com/products/matlab.html> - Accessed on Oct. 20, 2022.
- [56] João Gomes-Fonseca, Fernando Veloso, Sandro Queirós, Pedro Morais, António C. M. Pinho, Jaime C. Fonseca, Jorge Correia-Pinto, Estêvão Lima, and João L. Vilaça. Technical note: Assessment of electromagnetic tracking systems in a surgical environment using ultrasonography and ureteroscopy instruments for percutaneous renal access. *Medical Physics*, 47:19–26, 1 2020.
- [57] "WHO - GLOBOCAN Database", <https://gco.iarc.fr/today/home> - Accessed on Sep.8, 2022.
- [58] Richard Barr, Hindi, and Peterson. Artifacts in diagnostic ultrasound. *Reports in Medical Imaging*, 6:29, 6 2013.
- [59] Yuzhou Hu, Yi Guo, Yuanyuan Wang, Jinhua Yu, Jiawei Li, Shichong Zhou, and Cai Chang. Automatic tumor segmentation in breast ultrasound images using a dilated fully convolutional network combined with an active contour model. *Medical Physics*, 46:215–228, 1 2019.

- [60] Residual feedback network for breast lesion segmentation in ultrasound image, 2021.
- [61] Gelan Ayana, Kokeb Dese, and Se woon Choe. Transfer learning in breast cancer diagnoses via ultrasound imaging. *Cancers*, 13:738, 2 2021.
- [62] Eleonora Tagliabue, Diego Dall’Alba, Enrico Magnabosco, Chiara Tenga, Igor Peterlik, and Paolo Fiorini. Position-based modeling of lesion displacement in ultrasound-guided breast biopsy. *International Journal of Computer Assisted Radiology and Surgery*, 14:1329–1339, 8 2019.
- [63] Joerg Heil, Peter Sinn, Hannah Richter, André Pfob, Benedikt Schaefgen, André Hennigs, Fabian Riedel, Bettina Thomas, Marc Thill, Markus Hahn, Jens Uwe Blohmer, Sherko Kuemmel, Maria Margarete Karsten, Mattea Reinisch, John Hackmann, Toralf Reimer, Geraldine Rauch, and Michael Golatta. Responder - diagnosis of pathological complete response by vacuum-assisted biopsy after neoadjuvant chemotherapy in breast cancer - a multicenter, confirmative, one-armed, intra-individually-controlled, open, diagnostic trial. *BMC Cancer*, 18:1–7, 8 2018.
- [64] Michael Rosenthal, Andrei State, Joohee Lee, Gentaro Hirota, Jeremy Ackerman, Kurtis Keller, Etta D Pisano, Michael Jiroutek, Keith Muller, and Henry Fuchs. Augmented reality guidance for needle biopsies: An initial randomized, controlled trial in phantoms. *Medical Image Analysis*, 6:313–320, 9 2002.
- [65] David Asgar-Deen, Jay Carriere, Ericka Wiebe, Lashan Peiris, Aalo Duha, and Mahdi Tavakoli. Augmented reality guided needle biopsy of soft tissue: A pilot study. *Frontiers in Robotics and AI*, 7:72, 6 2020.
- [66] Pedro F. Gouveia, Joana Costa, Pedro Morgado, Ronald Kates, David Pinto, Carlos Mavioso, João Anacleto, Marta Martinho, Daniel Simões Lopes, Arlindo R. Ferreira, Vasileios Vavourakis, Myrianthi Hadjicharalambous, Marco A. Silva, Nickolas Papanikolaou, Celeste Alves, Fatima Cardoso, and Maria João Cardoso. Breast cancer surgery with augmented reality. *The Breast*, 56:14–17, 4 2021.
- [67] Shinichiro Kashiwagi, Yuka Asano, Wataru Goto, Tamami Morisaki, Masatsune Shibutani, Hiroaki Tanaka, Kosei Hirakawa, and Masaichi Ohira. Optical see-through head-mounted display (ost-hmd)-assisted needle biopsy for breast tumor: A technical innovation. *In Vivo*, 36:848–852, 3 2022.
- [68] "ACECUT BIOPSY NEEDLE PRODUCT INFORMATION TSK Laboratory, Japan", https://www.tsklab.co.jp/en/products/biopsy_needle/acecut.php - Accessed on Sep. 26, 2022.

- [69] "Artificial Intelligence Computing Leadership from NVIDIA", <https://www.nvidia.com/en-us/> - Accessed on Oct. 19, 2022.
- [70] "CUDA Toolkit - Free Tools and Training | NVIDIA Developer", <https://developer.nvidia.com/cuda-toolkit> - Accessed on Oct. 19, 2022.
- [71] Michael Garland, Scott Le Grand, John Nickolls, Joshua Anderson, Jim Hardwick, Scott Morton, Everett Phillips, Yao Zhang, and Vasily Volkov. Parallel computing experiences with cuda. *IEEE Micro*, 28:13–27, 7 2008.
- [72] Dmitri Priimak. Finite difference numerical method for the superlattice boltzmann transport equation and case comparison of cpu(c) and gpu(cuda) implementations. *Journal of Computational Physics*, 278:182–192, 12 2014.
- [73] Prajoona Valsalan, P. Sriramakrishnan, S. Sridhar, G. Charlyn Pushpa Latha, A. Priya, S. Ramkumar, A. Robert Singh, and T. Rajendran. Knowledge based fuzzy c-means method for rapid brain tissues segmentation of magnetic resonance imaging scans with cuda enabled gpu machine. *Journal of Ambient Intelligence and Humanized Computing*, pages 1–14, 5 2020.
- [74] Pralhad Gavali and J. Saira Banu. Deep convolutional neural network for image classification on cuda platform, 1 2019.
- [75] "Qt | Cross-platform software development for embedded & desktop", <https://www.qt.io/> - Accessed on Sep. 26, 2022.
- [76] "Home - OpenCV", <https://opencv.org/> - Accessed on Sep. 26, 2022.
- [77] Sergio Pereira, Adriano Pinto, Victor Alves, and Carlos A. Silva. Brain tumor segmentation using convolutional neural networks in mri images. *IEEE Transactions on Medical Imaging*, 35:1240–1251, 5 2016.
- [78] Margarida R. Ferreira, Helena R. Torres, Bruno Oliveira, Joao Gomes-Fonseca, Pedro Morais, Paulo Novais, and Joao L. Vilaca. Comparative analysis of current deep learning networks for breast lesion segmentation in ultrasound images. pages 3878–3881. IEEE, 7 2022.
- [79] Raul Ferrete Ribeiro, Joao Gomes-Fonseca, Helena R. Torres, Bruno Oliveira, Estela Vilhena, Pedro Morais, and Joao L. Vilaca. Deep learning methods for lesion detection on mammography images: a comparative analysis. pages 3526–3529. IEEE, 7 2022.

- [80] Asha A. Bhatt, Dana H. Whaley, and Christine U. Lee. Ultrasound-guided breast biopsies. *Journal of Ultrasound in Medicine*, 40:1427–1443, 7 2021.
- [81] "Polaris Vega ST - NDI", <https://www.ndigital.com/optical-measurement-technology/polaris-vega/polaris-vega-st/> - Accessed on Sep. 26, 2022.
- [82] Nathan Bluvol, Anat Kornecki, Allison Shaikh, David Del Rey Fernandez, Donald H. Taves, and Aaron Fenster. Freehand versus guided breast biopsy: Comparison of accuracy, needle motion, and biopsy time in a tissue model. *American Journal of Roentgenology*, 192:1720–1725, 6 2009.

Support

The OncoNavigator project was funded by the projects "NORTE-01-0145-FEDER-000045" and "NORTE-01-0145-FEDER-000059", supported by Northern Portugal Regional Operational Programme (NORTE 2020), under the Portugal 2020 Partnership Agreement, through the European Regional Development Fund (FEDER). It was also funded by national funds, through the FCT (Fundação para a Ciência e a Tecnologia) and FCT/MCTES in the scope of the project UIDB/05549/2020, UIDP/05549/2020 and LASI-LA/P/0104/2020.

